Quaternary upper plate deformation in coastal Oregon

Harvey M. Kelsey *Department of Geology, Humboldt State University, Arcata, California 95521*
Robert L. Ticknor *74 Russell Avenue, Watertown, Massachusetts 02172*
James G. Bockheim *Department of Soil Science, University of Wisconsin, Madison, Wisconsin 53706*
Clifton E. Mitchell *Science Department, Lane Community College, Eugene, Oregon 97403-0640*

ABSTRACT

The leading edge of the North American plate along the Cascadia subduction zone is deforming and rotating clockwise as a consequence of both underthrusting of the Gorda–Juan de Fuca plate and collision of the North American plate with the Pacific plate. The details of late Quaternary (≤125 ka) upper-plate deformation resulting from these plate interactions are largely obscured because the most recent deformation overprints earlier deformation in the Tertiary rocks of the Coast Range. However, by mapping uplifted wave-cut platforms formed during times of high sea level in the past ≈500 000 yr, we identify faults and folds active in the late Quaternary in central coastal Oregon. Through along-coast correlation of these platforms using elevation and soil development, we infer that several major faults have vertically offset platforms at rates as high as 0.6 m/k.y. for the past 125 k.y. We regionally extend our analysis by incorporating all known faults and folds in southern and central coastal Oregon that deform wave-cut platforms. Most platforms along the southern and central Oregon coast have been uplifted at rates of 0.1–0.3 m/k.y. since the late Pleistocene; however, platform uplift rates approach 1 m/k.y. in the vicinity of faults. The trend and distribution of these upper-plate coastal faults are consistent with their interpreted role as left-lateral, strike-slip, block-bounding structures accommodating clockwise rotation. We speculate that these upper-plate faults have a component of dip slip because of their association, in many instances, with localized uplift. If these faults bound rotating blocks, the dip-slip component of displacement may be either contractional or extensional, depending on the orientation of the fault relative to the north-south trend of the plate margin.

INTRODUCTION

Studies in Holocene tidal-wetland deposits along the Cascadia subduction zone in northern California, Oregon, Washington, and British Columbia have shown that the Cascadia margin has generated plate-boundary earthquakes of magnitude 8 or larger (Atwater, 1987, 1992; Darienzo and Peterson, 1990; Clarke and Carver, 1992; Clague and Bobrowsky, 1994; Darienzo et al., 1994; Atwater et al., 1995). Among the uncertainties concerning the nature of the plate boundary are the times and maximum size of plate-boundary earthquakes and the tectonic role of folds and faults in the upper plate. This paper addresses the second question by capitalizing on a unique late Pleistocene datum—the wave-cut platform—that records uplift, folding, and faulting of the upper plate in the past 100 000 yr. Wave-cut platforms provide a catalog of the location and movement history of upper-plate structures, thereby contributing to the development and assessment of kinematic models of upper-plate deformation.

In the first part of this report we describe geologic structures that have been active in the Holocene and/or late Quaternary within the upper plate in the onshore region of coastal central Oregon (Fig. 1). Onshore upper-plate structures active in the late Quaternary have been recognized elsewhere in coastal Oregon (Adams, 1984; Kelsey, 1990; Muhs et al., 1990; McInelly and Kelsey, 1990; Kelsey and Bockheim, 1994), but we focus on the central Oregon coast because these structures have not been described. In the latter part of the paper, we will address all active upper-plate structures in coastal Oregon, where we define "active" structures as those that deform surfaces cut in the past 125 k.y. or sediments deposited in the past 125 k.y. In our analysis of upper-plate deformation, we primarily consider the data set consisting of elevations of late Pleistocene (≤125 ka) wave-cut platforms and secondarily a data set consisting of level-line surveys over an ≈45 yr period along western Oregon highways. We also draw from several other published data sets that document differential vertical displacement in the upper plate during the Quaternary.

This study attempts to demonstrate the youthfulness of several upper-plate structures, to constrain their style of deformation, and to relate this deformation to plate tectonics of the Cascadia margin. We hypothesize that upper-plate structures in central coastal Oregon are active, that they deform as part of the broad deformation zone that bounds the western margin of the North American plate, and that these structures are compatible with a prevailing upper-plate deformation model of dextral shear and clockwise rotation. We test these hypotheses through the following approaches. Upper-plate structures are recognized on the basis of deformation of marine terraces and geodetic leveling. Age assignments for marine terraces are determined through analyses of the degree of soil development on marine terraces and correlation of these soils to those on marine terraces elsewhere in coastal Oregon that have numerical ages. Fault style and fault-slip rate are constrained by mapping of fault trends and by evaluating magnitude of fault offset of marine platforms. Using all upper-plate active structures in coastal Oregon as a data base, we evaluate whether a model of dextral shear and clockwise rotation of the upper plate is compatible with late Pleistocene faulting and folding along the Oregon coast of the Cascadia margin.

UPPER PLATE GEOLOGY IN CENTRAL COASTAL OREGON

Regional Bedrock Geology of the Oregon Coast Range

The Oregon Coast Range consists of a tectonically elevated belt of crust lying 150–200 km

GSA Bulletin; July 1996; v. 108; no. 7; p. 843–860; 11 figures; 8 tables.

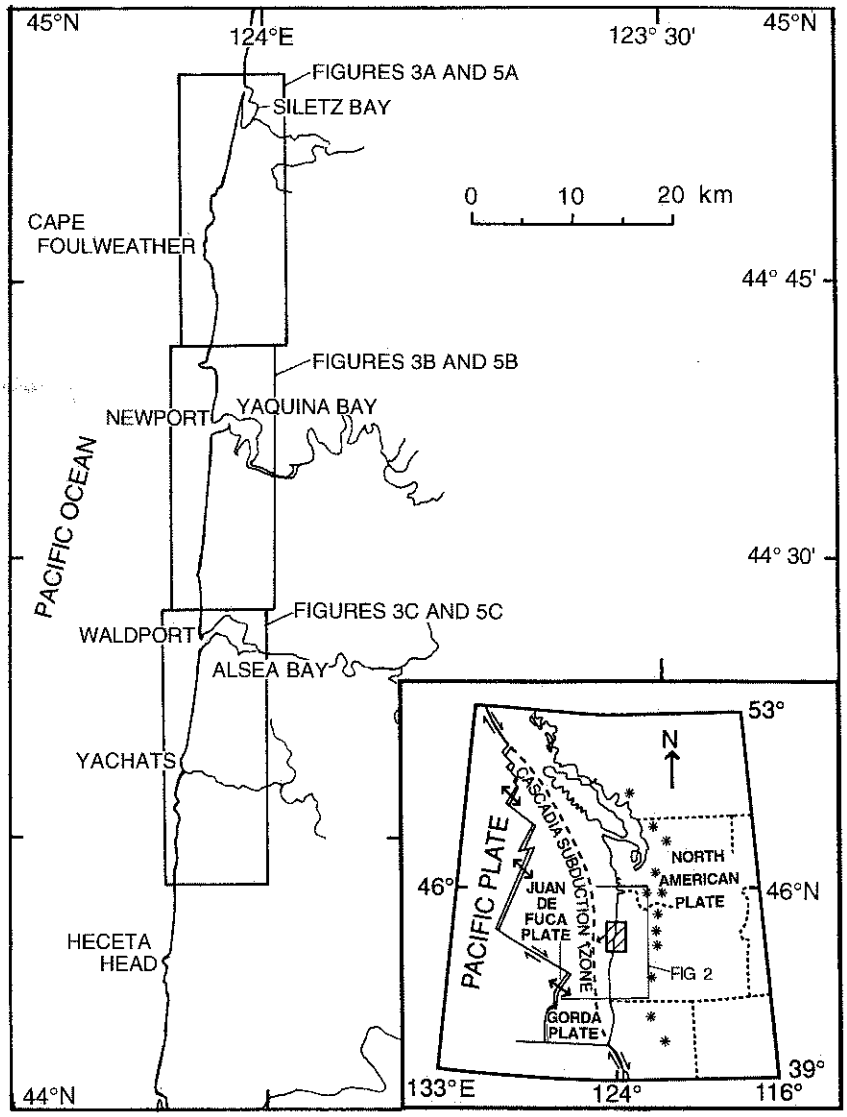

Figure 1. Location map for the central Oregon coast. Inset shows regional plate tectonic setting; asterisks denote volcanoes of the Cascade Range.

east of the deformation front of the Cascadia subduction zone and overlying the subducted Juan de Fuca plate. The central and northern Oregon coast consists primarily of westward-dipping Tertiary marine and volcanic sedimentary rocks, mainly Eocene in age, intruded by basalt (Snavely et al., 1969, 1976a, 1976b, 1976c; Walker and MacLeod, 1991; Wells et al., 1994). These west-dipping Tertiary sedimentary rocks form the west flank of a structural high that defines the Coast Range from latitude 43° north to the Columbia River.

The youngest Tertiary strata in the Coast Range, of Oligocene and Miocene age, are exposed in central coastal and north coastal Oregon (unit Tom; Fig. 2). On the basis of the outcrop areas of these strata, we infer that the magnitude of uplift of crustal rocks (that is, uplift of rock as opposed to surface uplift; England and Molnar, 1990) along the Oregon coast is at a minimum near Yaquina Bay and near Netarts Bay, and also reaches a minimum within the embayment at the mouth of the Columbia River (Fig. 2). The greatest magnitude of rock uplift in the Oregon Coast Range occurs in southern Oregon, where Mesozoic and Paleozoic metasedimentary rocks, volcanic rocks, and plutonic rocks of the Klamath Mountains are exposed (Fig. 2).

Quaternary Tectonics of the Oregon Coast and Continental Margin

The central Oregon coast is 100 to 110 km east of the deformation front at the western edge of the Cascadia subduction zone. The most prominent tectonic features of the continental margin area between the coast and the deformation front are a set of late Quaternary thrust faults and folds that extend parallel to the deformation front (Kulm and Fowler, 1974; Peterson et al., 1986; Goldfinger et al., 1992b). The thrust faults extend from the deformation front on the west to the top of the continental rise on the east (Fig. 2). Farther east on the shelf, folds predominate over thrust faults. Another prominent feature of the offshore continental margin is a set of east-southeast–trending high-angle faults (Wecoma fault, Fault B, Fault C; Fig. 2) that extend from the abyssal plain eastward across the deformation front to the top of the continental rise (Applegate et al., 1992; Goldfinger at al., 1992a, 1992b). The Wecoma fault offsets the base of the continental slope in a left-lateral strike-slip sense; the average slip rate is 5–12 mm/yr in the past 10–24 k.y. (Applegate et al., 1992). These faults can be traced farther eastward across the shelf and project toward the coastal zone between Alsea and Siletz Bays (Fig. 2). A second set of west-northwest–trending faults projects from the shelf onto the coast in the vicinity of Netarts Bay (Fig. 2).

Within the two major embayments along the central Oregon coast, Alsea Bay and Yaquina Bay (Fig. 1), multiple buried marsh soils are preserved, some in association with sand layers deposited directly on the buried soils. This stratigraphic sequence has been interpreted as a late Holocene record of repeated coseismic submergence events, some events followed by deposition of sand due to a tsunami (Peterson and Darienzo, 1988, 1990; Darienzo, 1991; Darienzo et al., 1994). These workers hypothesize that the submergence events are due to episodic megathrust earthquake events along the Cascadia subduction zone. Similar sequences of interbedded peat and mud have been described in estuaries in southern British Columbia (Clague and Bobrowsky, 1994), southern Washington (Atwater, 1987, 1992), northern Oregon (Darienzo and Peterson, 1990), southern Oregon (Nelson, 1992; Kelsey et al., 1993), and northern California (Clark and Carver, 1992), opening the possibility that all or most of these marshes may have undergone repeated synchronous regional coseismic submergence (Peterson and Darienzo, 1988, 1996; Darienzo et al., 1994).

MARINE TERRACES ALONG THE CENTRAL OREGON COAST

Introduction

Bedrock shore platforms (Bradley and Griggs, 1976) that form during interglacial sea-

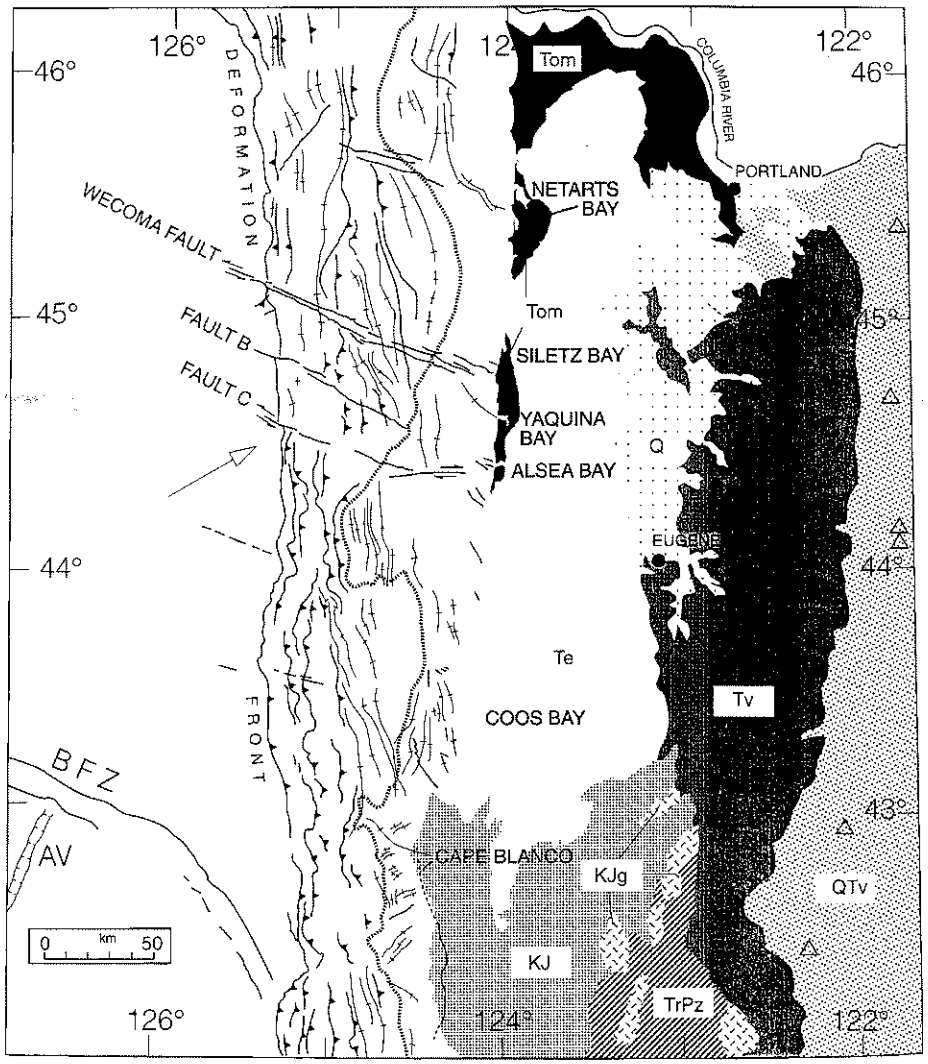

Figure 2. Tectonic map for continental shelf and rise of offshore Oregon and generalized geologic map for western Oregon west of the Cascade Mountains. Offshore data from Goldfinger et al. (1992b); onshore data from Walker and MacLeod (1991). All structures displace Pleistocene or younger sediments. This paper focuses on the late Quaternary deformation along the Oregon coast in the vicinity of Alsea, Yaquina, and Siletz Bays. Sites along the Oregon coast where late Holocene coseismic subsidence has been reported include, from north to south, Netarts Bay (Darienzo and Peterson, 1990), Siletz and Yaquina Bays (Darienzo et al., 1994), Coos Bay (Nelson, 1992), and the Sixes River at Cape Blanco (Kelsey et al., 1993). Bold dashed line is edge of continental shelf; bold solid line is steeply dipping fault; bold solid line with teeth is thrust fault with teeth on upper plate; thin solid lines with short cross bars are fold axes. AV is axial valley of the spreading ridge separating the Pacific plate to the west from the Gorda plate to the east. BFZ is Blanco fracture zone. The Juan de Fuca plate is bounded by the BFZ on the south and the deformation front on the east. The North American plate occurs east of the deformation front. The young (ca. 19 Ma) Juan de Fuca plate is obliquely subducting under the North American plate at ≈40 mm/yr (Riddihough, 1984). Explanation of geologic symbols: Q, Quaternary sedimentary fill in the Willamette valley; QTv, Quaternary and Tertiary volcanic rocks and volcaniclastic sediments of the Cascade Mountains; Tv, Tertiary volcanic rocks east of the Willamette valley and the Coast Range; Tom, Tertiary Oligocene and Miocene sedimentary and volcanic rocks of the Coast Range; Te, Tertiary Eocene volcanic and sedimentary rocks of the Coast Range; KJ, Cretaceous and Jurassic rocks of the Klamath Mountains; KJg, intrusive igneous rocks of the Klamath Mountains; TrPz, Triassic and Paleozoic rocks of the Klamath Mountains. Triangles denote volcanoes of the Cascade Range.

level highstands (Bloom et al., 1974) can serve as reference horizons from which to estimate late Quaternary deformation (Adams, 1984; Lajoie, 1986; Merritts and Bull, 1989; Kelsey, 1990; McInelly and Kelsey, 1990; Clarke and Carver, 1992). Such platforms are preserved along the central Oregon coast in the form of uplifted marine terraces. Each terrace is underlain by a thin (2–40 m) veneer of mostly marine sediment that covers the wave-cut platform.

We identified a set of six marine terraces on the central Oregon coast (Ticknor, 1993) (Fig. 3 and Table 1). Terraces are preserved discontinuously, range in elevation from sea level to 153 m and extend as much as 3 km inland. The younger and better preserved terraces typically form narrow strips ranging from <100 to ≈800 m in width. In the vicinity of Yaquina and Alsea Bays, the terraces are widest, attaining widths up to 2000 m.

Marine terraces were differentiated by terrace elevation, wave-cut platform elevation, terrace back-edge relief, and cover-bed stratigraphy (Table 1), as well as by degree of soil development. Platform elevations were measured wherever possible. Measurement sites were located on 1:24 000 maps using aerial photographs. Elevations were read off the maps with an accuracy of one-half the contour interval, which is ±6 m. Altimeter surveys (error ±3.3 m) were employed for the lowest wave-cut platforms, wherever ties to permanent benchmarks could be established.

Sediments that underlie the terraces are typically high-energy nearshore marine deposits capped by beach sand. Vegetated relict sand dunes commonly cover part of the beach deposits. These deposits are most prevalent in the vicinity of Alsea Bay, where hummocky dunal topography is characteristic of the surfaces of the lower terraces.

Previously reported ages for uplifted marine terraces in central coastal Oregon are limited to the vicinity of Yaquina Bay. Kennedy (1978) and Kennedy et al. (1982) assigned an age of 125 ka (oxygen isotope stage 5e) to cover sediments above the wave-cut platform at Hinton Point (also named Idaho Point) on the south side of Yaquina Bay (Fig. 3). This age assignment is based on a warm-water affinity of the fossil mollusk shells, in conjunction with amino acid enantiomeric (D:L) ratios for fossil shells. In contrast, amino acid D:L ratios for shells collected from terrace sediments above a wave-cut platform at Yaquina Bay State Park, on the north side of Yaquina Bay, correlate with amino acid D/L ratios from southern Oregon, and suggest an age of 80–85 ka (oxygen isotope 5a) (Kennedy, 1978; Kennedy et al., 1982). The difference in D:L ratios between

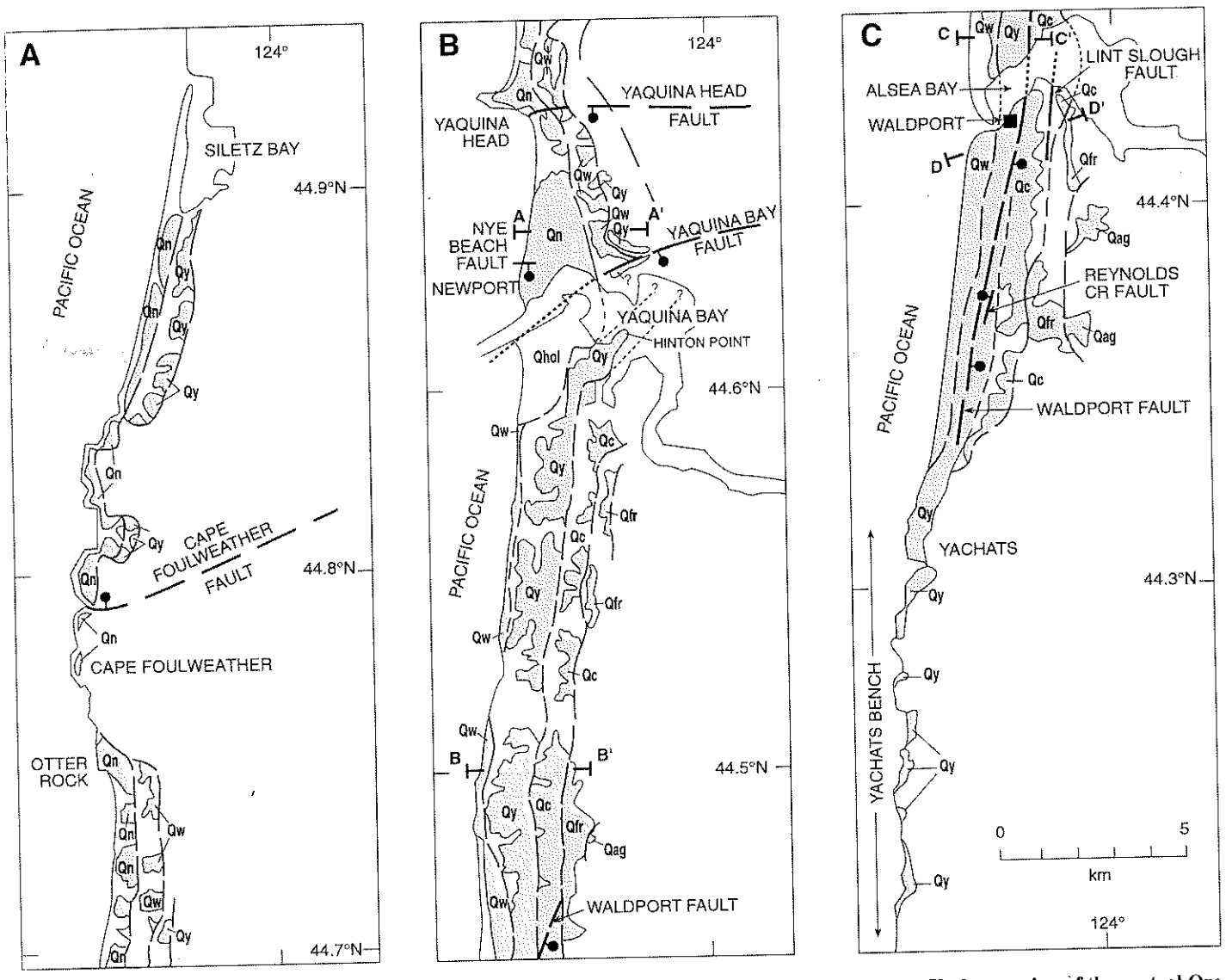

Figure 3. Quaternary marine terrace sediments, and faults that offset these sediments, in Newport-Yachats region of the central Oregon coast. (A, B, and C) Northern, middle, and southern portion of study area, respectively. Late Quaternary sediments, from youngest to oldest: Qhol, Holocene beach and dune sands southeast of Yaquina Bay; Qn, Newport terrace sediments; Qw, Wakonda terrace sediments; Qy, Yachats terrace sediments; Qc, Crestview terrace sediments, Qfr, Fern Ridge terrace sediments; Qag, Alder Grove terrace sediments. The eastern boundary of each unit of terrace sediment is the estimated position of the terrace back edge (shoreline angle); back edge is solid where located and dashed where inferred. Bold lines show faults that offset late Pleistocene marine terrace deposits, with solid ball on downthrown side. See Figure 4 for cross sections A–A′ through D–D′. Cape Foulweather fault is one of the faults mapped by Snavely et al. (1976c) and is selected as a candidate structure to account for offsets in the elevation of marine platforms along this portion of the coast. Yaquina Head fault from Snavely et al. (1976b). Yaquina Bay fault is inferred on the basis of research reported in this paper; the continuation of this fault to the east of Yaquina Bay was mapped by Snavely et al. (1976b). The Waldport, Reynolds Creek, and Lint Slough faults are identified on the basis of terrace platform offsets reported in this paper.

Yaquina Bay State Park and Hinton Point is approximately the same as the difference between 80 and 125 ka deposits in southern California (Kennedy, 1978; Kennedy et al., 1982).

These ages raise a problem about the terrace chronology in the vicinity of Yaquina Bay. Using the Kennedy et al. (1982) age assignments, the second-lowest terrace south of Yaquina Bay is ca. 125 ka and the lowest terrace north of Yaquina Bay is ca. 80 ka; yet the shore platforms of these two terraces on opposing sides of the bay are approximately equal in elevation. Either the age assignments of Kennedy et al. (1982) are in error, or a fault displaces the terraces across Yaquina Bay.

Distribution and Morphology

On the basis of the presence and number of marine terraces, we divided the central Oregon coast into three reaches with respect to marine terrace preservation: the reach north of Yaquina Bay (Siletz Bay to Newport); the reach between Yaquina Bay and Yachats (Newport to

TABLE 1. MARINE TERRACES OF THE CENTRAL OREGON COAST

Terrace name	Preservation and occurrence	Platform elevation (m)	Backedge height (m)	Cover sediment thickness (m)	Assigned age (ka)*	Faults cutting terrace deposits
Newport	Only occurs north of Yaquina Bay; well preserved; extensive	<0–40	28–40	4–19	80	Yaquina Head; Yaquina Bay
Wakonda	Regionally extensive, moderately dissected	<0–85	6–49	4–32†	105	Yaquina Head; Yaquina Bay
Yachats	Regionally extensive; moderately dissected	<0–109	5–28	4–30†	125	Waldport; Yaquina Bay
Crestview	Regionally extensive south of Yaquina Bay; highly dissected	28–82	12–47	10–27†	≥200	Waldport; Lint Slough
Fern Ridge	Remnants preserved near Yaquina and Alsea Bays, highly dissected	66–100	15–40	2–16	>200	
Alder Grove	Remnants preserved near Alsea Bay; highly dissected	94–153	N.D.§	8–44	>200	

*Assigned ages are based on Kennedy (1978), Kennedy and others (1982) and terrace correlation (Table 7).
†In areas of paleo-sand dunes in vicinity of Alsea Bay, cover bed thickness in places exceeds upper limit.
§N.D., no data.

Yachats); and the reach south of Yachats (Yachats to Heceta Head).

Siletz Bay to Newport. Three marine terraces are preserved in this coastal reach (Fig. 3). The lowest terrace, the Newport terrace (Fig. 4A), is extensively preserved directly north of Yaquina Bay and discontinuously preserved from Cape Foulweather to Siletz Bay. The average width of the terrace is ≈500 m, and the terrace reaches its maximum width (1300 m) immediately north of Yaquina Bay. Platform elevations range from 0 to 45 m (Table 1).

The middle terrace is highly dissected and only preserved from Newport north to Otter Rock (Fig. 3); the platform underlying this terrace ranges in elevation from 59 to 85 m (Table 1). The highest terrace in this coastal reach is discontinuously preserved from Yaquina Bay to Siletz Bay (Fig. 3), and the underlying platform elevations range from 14 to 109 m.

Newport to Yachats. Five marine terraces are preserved in this coastal reach (Fig. 3). The lowest marine terrace is the Wakonda terrace (Fig. 4, A and B). Between Yaquina and Alsea Bays, the Wakonda wave-cut platform is exposed in the sea cliffs just above the modern beach; a discontinuous back edge is preserved just inland from the beach (Figs. 3 and 4). Around Alsea Bay, the terrace tread reaches >500 m in width, and the back edge is farther inland and largely obscured by active and vegetated dunes (Fig. 4D). South of Alsea Bay, the Wakonda platform is well preserved and gradually descends in altitude to the south, becoming submerged just north of Yachats (Fig. 3).

The second terrace in this coastal reach, the Yachats terrace, is well preserved from Yaquina Bay south to Yachats (Fig. 3). Platform elevations range from 14 to 44 m (Table 1). In general, the Yachats back edge is well preserved; however, in the vicinity of Alsea Bay, the back edge is poorly defined where it is concealed by thick Quaternary dune deposits and offset by north-south–trending faults (Table 1; Fig. 4, C and D).

The third-highest terrace in this coastal reach, the Crestview terrace, is preserved from the south side of Yaquina Bay to north of Yachats (Fig. 3). The Crestview platform is downwarped in the vicinity of Alsea Bay. Variable tread relief and isolated sandy road cuts suggest an extensive dunal cap on Crestview marine terrace sediments.

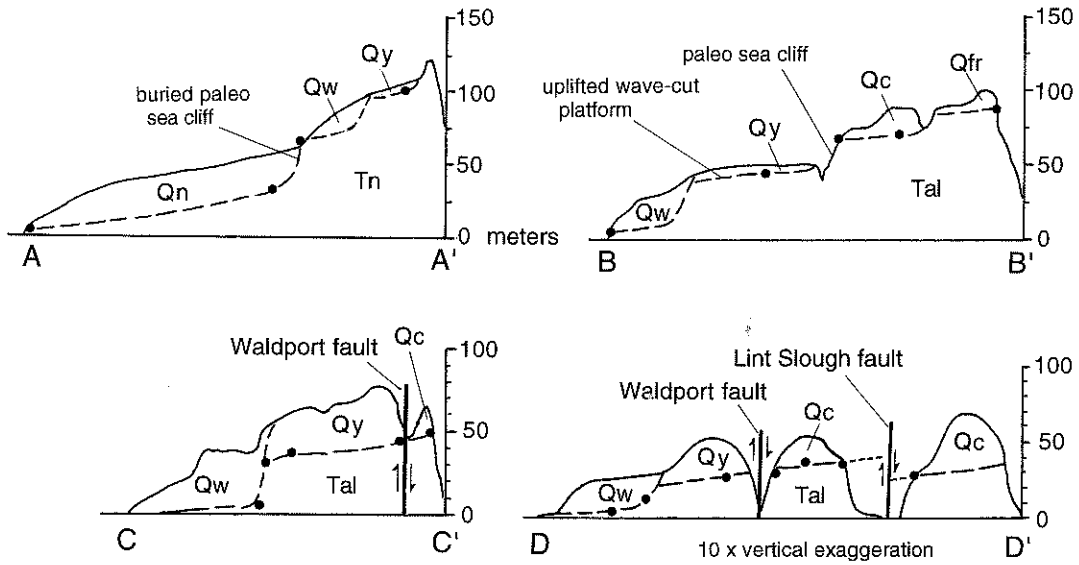

Figure 4. Topographic cross sections of marine terraces; vertical exaggeration is 10×. See Figure 3 for locations. Qn, Newport terrace sediments; Qw, Wakonda terrace sediments; Qy, Yachats terrace sediments; Qc, Crestview terrace sediments; Qfr, Fern Ridge terrace sediments; Tal, Alsea Formation siltstone and fine sandstone (Snavely et al., 1976a); Tn, Nye Mudstone (Snavely et al., 1976b). Dots are measured elevations projected onto the cross-section lines from the north or south; no elevations were projected from distances >1500 m. Note that the Newport terrace is above sea level north of Yaquina Bay (A–A′) and is submerged south of Yaquina Bay (B–B′; C–C′; D–D′). The unusually thick terrace cover sediments in the vicinity of Alsea Bay (C–C′) reflect paleo-sand dunes on top of marine terrace sediments.

The oldest and highest terraces, the Fern Ridge and Alder Grove terraces, are preserved only in the vicinity of Alsea Bay on hill tops and ridge crests (Fig. 3). The platforms of both these terraces are tilted to the south.

Yachats to Heceta Head. South of Yachats, a single marine terrace crops out as a low bench, informally referred to as the Yachats Bench (Fig. 3). Platform elevations along the Yachats Bench decrease to the south and range from 13 to 0 m. The platform becomes submerged just north of Heceta Head (Fig. 1). Cover sediments on the Yachats Bench consist of beach sand that is in almost all instances overlain by eolian sand, debris flows, or both.

Marine Terrace Soils

We defined a soil chronosequence (a sequence of soils that differ in certain properties primarily as a function of time) for central Oregon coastal marine terraces and then used the chronosequence as a tool to correlate marine terraces across the three coastal reaches and to correlate the terraces to flights of marine terraces at other localities on the Cascadia margin. These correlations are the basis for identifying long-term, permanent vertical deformation along the coast. Ticknor (1993) provided more thorough discussion of soil properties, laboratory analyses of particle size, and aspects of pedogenesis for the central Oregon coast. The parent material for all the soils is unconsolidated Pleistocene beach or dune sand. Some soils described on the Yachats bench developed on basalt-rich debris flow deposits that overlie beach sand.

Field-identifiable soil properties that are both time dependent and can be used to distinguish the terraces include the depth to the Cox horizon (oxidized parent material), the thickness of the clay-enriched (Bt) horizon, the estimated maximum percent clay, and maximum clay skins. From these properties, we assigned development stages for the soils (Table 2) (Kelsey and Bockheim, 1994).

Soils were examined at 56 sites (Fig. 5) on the 6 marine terraces within the study area. Soil pits were excavated for 14 sites to a depth of 2 m, with continued augering down to the Cox horizon. Soils at 42 other sites were described from samples obtained with a 7.5-cm-diameter bucket auger. Soil data are presented separately for the three subregions: Siletz Bay to Newport (Table 3), Newport to Yachats (Table 4) and Yachats to Heceta Head (Table 5).

Soil properties change as a function of time for the six terraces (Fig. 6; Tables 3 and 4). Significant aspects of the Figure 6 data are: the average depth to the C horizon steadily increases (Fig. 6A); the Bt horizon thickness increases almost linearly for the first five terraces (Fig. 6B); the average estimated percent clay increases along with Bt thickness from ≈30% on the youngest two terraces to slightly >40% on the next three older terraces (Fig. 6C); and the development stage increases almost linearly from 1.8 on the youngest terrace to 6.0 on the next to oldest terrace (Fig. 6D). It is also clear from Figure 6 that soils on the two oldest terraces cannot be distinguished from each other. Distinctions between these two terraces, however, were not critical for the platform correlations.

TABLE 2. DEVELOPMENT STAGES OF SOILS ON ELEVATED MARINE TERRACES ALONG THE CENTRAL AND SOUTHERN OREGON COAST

Development stage	Depth to Cox (m)	B horizon hue	Bt (cm) thickness	Maximum B horizon texture* (% clay)†	Maximum clay films§
1	0.8–1.4	7.5–10YR	0	sil, l, sl (<30)	1–3npfpo
2	1.0–1.4	7.5YR	<50	sicl, cl, scl (30–40)	2–3n-mkpfpo
3	1.0–1.7	7.5YR	<50	sicl, cl, scl (30–40)	2–3mkpfpo
4	1.4–1.8	5–7.5YR	50–100	sicl, sic, cl, c (35–42)	3–4mkpfpo
5	1.9–2.8	5–7.5YR	100–200	sic, c (40–58)	3–4mk-kpfpo
6	2.6–4.5	5YR	>200	sic, c (40–65)	3–4mk-kpfpo
7	3.2–>4.5	2.5YR	>200	sic, c (45–65)	3–4mk-kpfpo

*S, sand; l, loam; sl, sandy loam; sil, silt loam; sicl, silty clay loam; sic, silty clay; cl, clay loam; c, clay. Abbreviations follow Soil Survey Staff (1975).

†We estimated percent clay for each horizon at each soil locality during field work. We have confidence in our ability to estimate clay content in the field because we obtained a significant correlation ($R = 0.81$; $p \leq 0.01$) between percent clay measured in the field and percent clay measured in the laboratory (28 samples).

§Notations for clay films: number denotes extent of ped faces covered by film: 1, 5%–25%; 2, 25%–50%; 3, 50%–90%; 4, >90%; n, thin; mk, moderately thick; k, thick; pf, film on ped face; po, film lines the pores. Abbreviations follow Soil Survey Staff (1975).

In the vicinity of Alsea Bay, development stages for soils on terrace sediments were conspicuously lower than the surrounding regions. Thirteen soil sites, which were notably underdeveloped, are not included in Table 4 or in Figures 5 and 6, and were not used for relative dating. Soils at these sites have developed on extensive sand dune deposits. Prolonged eolian activity on terrace surfaces in proximity to Alsea Bay is the likely explanation for the poorly developed soils.

In summary, the lowermost four marine terraces can be distinguished from one another on the basis of field-identifiable soil properties. The soils on Fern Ridge and Alder Grove terraces, in contrast, are old enough for the soils to have developed to such an extreme that distinguishing between the two is difficult (terrace 5 versus terrace 6 in Table 4). However, their relative ages are established based on elevation of the respective terraces.

Correlation of Marine Terraces on Either Side of Yaquina Bay Using Soils: The Yaquina Bay Fault

Matching of marine terraces across Yaquina Bay is necessary for evaluation of the hypothesis that a fault underlies the bay. A sequence of three terraces is preserved in the first 10 km north of the bay and a sequence of five terraces is preserved in the first 10 km south of the bay (Figs. 3 and 7A). We compared soil descriptions for the lowest three terraces 10 km south of the bay with the lowest three terraces 10 km north of the bay to evaluate the possible matches (Fig. 7B and Table 6). The best match based on soil properties (Fig. 7C and Table 6) indicates that the highest terrace north of Yaquina Bay can reasonably be matched with either the second- or third-highest terrace south of the bay. However, the only set of terrace matches entirely consistent with the soil data is the one that matches the highest (third) terrace north of the bay to the second-highest terrace south of the bay (Fig. 7D).

Matching of wave-cut platforms across Yaquina Bay shows that correlative platforms occur at different elevations on opposite sides of the bay, and the preferred match of terraces can only be accommodated if a fault beneath Yaquina Bay displaces the platforms up to the north (Figs. 7D and 8). A fault with the same sense of displacement, situated underneath

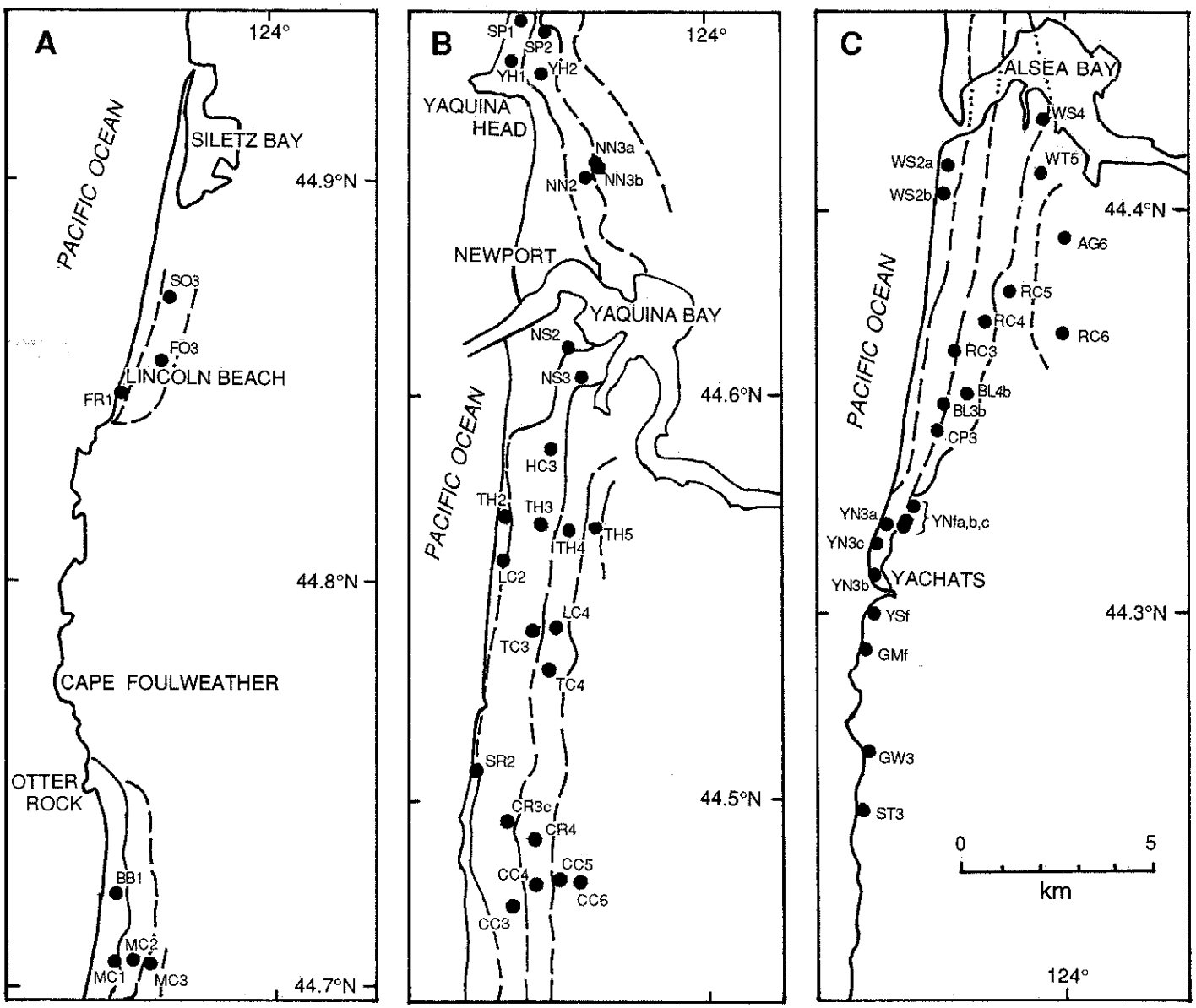

Figure 5. Maps showing sample sites for soil descriptions on marine terraces. (A, B, and C) The northern, central, and southern portions of the study area, respectively (see Fig. 1). Lines that are subparallel to, but east of, the coastline denote marine terrace back edges (shoreline angles); they are solid where exactly located and dashed where approximately located. The number in the alphanumeric soil code identifies the terrace: 1, Newport; 2, Wakonda; 3, Yachats; 4, Crestview; 5, Fern Ridge; 6, Alder Grove. Soil codes with lower-case f are sites where the soil parent material is debris flow deposits overlying the Yachats terrace. Tables 3, 4, and 5 provide summaries of soil properties at each sample site.

Yaquina Bay, is also required for the Kennedy et al. (1982) assignment of correlation ages for the same terraces. A consequence of the terrace match across Yaquina Bay is that the Newport terrace, which has the least-developed soil, is only exposed north of the bay and is submerged south of the bay due to fault displacement. Because five terraces are preserved south of Yaquina Bay where the youngest terrace is missing, there are six uplifted marine terraces along the central Oregon coast (Table 1).

The terrace data provide limited information from which to infer the trend of a fault underlying Yaquina Bay; however, Snavely et al. (1976b) identified an east-northeast–trending fault on the eastern shore of Yaquina Bay that offsets lower Miocene mudstone and has the same sense of displacement as the fault we infer to underlie the bay. We therefore prefer an east-northeast trend to the inferred fault beneath Yaquina Bay (Fig. 3) in order for our inferred fault and the fault of Snavely et al. (1976b) to be the same structure. This fault trace cuts marine terrace deposits at the north end of Yaquina Bay; unfortunately, the terrace remnant on the south side of the fault trace is too poorly preserved to be matched with either

TABLE 3. SUMMARY OF SOIL PROPERTIES USED AS RELATIVE AGE INDICATORS IN THE SILETZ BAY TO NEWPORT AREA

Terrace locality	Bt horizon thickness (cm)	B horizon hue	Depth to Cox (cm)	Maximum B horizon texture*	Maximum estimated (% clay)*	Maximum clay films*	Development stage
FR1	0	5YR	76	s	0	0	1
BB1	0	10YR	129	sicl	37	1mkpf	2
MC1	51	2.5YR	108	cl	30	2kpf	2
SP1	32	10YR	117	cl	30	3mkpf	2
YH1	0	N.D.†	93	sl	18	1npf	1
Average	21	10YR	112	sicl	29	1-2mkpf	1.6
MC2	84	10YR	145	sicl	34	3kpf	4
SP2	0	7.5YR	188	fsl	18	3npf	1
YH2	38	N.D.†	73	l	N.D.†	2npo	3
NN2	>92	10YR	>263	sicl	38	4mkpf	4
Average	>54	7.5–10YR	>168	sicl	30	3mkpf	3.0
SO3	272	10YR	>370	sic	40	4mkpf	4.5
FO3	447	10YR	460	sicl	36	3mkpf	4.5
MC3	66	10YR	184	sicl	35	3kpf	4
NN3b	325	7.5YR	430	sic	50	4mkpf	6
NN3c	>246	10YR	>313	sic	50	4kpf	6
Average	>212	7.5–10YR	>309	sic	45	4mkpf	5.0

*See Table 2 for explanations.
†N.D., no data.

TABLE 4. SUMMARY OF SOIL PROPERTIES USED AS RELATIVE AGE INDICATORS IN THE NEWPORT TO YACHATS AREA

Terrace locality	Bt horizon thickness (cm)	B horizon hue	Depth to Cox (cm)	Maximum B horizon texture*	Maximum estimated (% clay)*	Maximum clay films*	Development stage
NS2	65	N.D.†	145	sicl	N.D.†	2mkpf	4
TH2	30	N.D.†	100	sicl	N.D.†	3npf	3
LC2	0	5YR	82	N.D.†	N.D.†	N.D.†	1
SR2	0	5YR	80	sil	25	2npf	1
WS2a	36	N.D.†	107	sicl	N.D.†	2npf	3
WS2b	47	10YR	107	cl	35	3mkpf	3
Average	30	7.5YR	103	sicl	30	2–3n-mkpf	2.5
NS3	71	N.D.†	145	sicl	N.D.†	3kpf	4
HC3	94	7.5YR	170	sic	42	4mk-kpf	4
TH3	150	N.D.†	>245	sic	40	3mkpf	5
TC3	165	N.D.†	>279	sic	40	3mkpf	5
CR3c	50	7.5–10YR	107	c	42	3mk-kpf	3
CC3	31	10YR	125	cl	28	2npo	3
RC3	45	10YR	84	cl	32	4npf	3
BL3b	159	10YR	252	c	58	4kpf	5
CP3	27	10YR	84	sic	44	4mkpf	3
YN3a	82	N.D.†	205	sicl	N.D.†	2npf	4
YN3b	65	5–7.5YR	150	sicl	38	3mkpf	3
YN3c	44	10YR	111	sicl	40	4mkpf	3
Average	>108	10YR	>163	sic	40	3mkpf	3.8
TH4	69	N.D.†	138	sicl	N.D.†	3mkpf	4
LC4	61	10YR	140	sic	42	3mkpf	4
TC4	202	N.D.†	>240	sic	42	4mkpf	5
CR4	100	N.D.†	190	sicl	N.D.†	2npf	5
CC4	58	10YR	104	cl	30	2mkpf	3
WS4	291	10YR	>407	sicl	40	4mkpf	6
RC4	148	7.5YR	190	sic	40	4kpf	5
BL4b	266	10YR	333	c	55	4mk-kpf	6
Average	151	10YR	>227	sic	43	3mkpf	4.8
TH5	>180	N.D.†	>230	sic	42	3kpf	6
CC5	140	7.5–10YR	>360	sic	41	3kpf	6
WT5	210	10YR	255	sic	45	4kpf	6
RC5	>523	10YR	>688	sic	45	4kpf	6
Average	>263	10YR	>308	sic	43	3–4pf	6.0
CC6	137	7.5–10YR	200	sic	42	3mk-kpf	5
AG6	>205	10YR	>280	cl	34	3mkpf	6
RC6	>190	7.5YR	>525	sicl	37	3kpf	6
Average	>177	7.5–10YR	>335	sicl	38	3mk-kpf	5.7

*See Table 2 for explanations.
†N.D., no data.

of the candidate marine terraces—Wakonda or Yachats—across the fault to the north.

Assignment of Ages to Marine Terraces Through Correlation to Other Oregon Localities

We can assign ages to the central Oregon terrace sequence on the basis of correlation of the sequence to marine terraces in south coastal Oregon. In southern Oregon, marine terraces are extensively preserved on several headlands (Griggs, 1945; Janda, 1969; Kelsey, 1990; McInelly and Kelsey, 1990, Kelsey and Bockheim, 1994). We correlate the central and southern coastal terraces on the basis of the following evidence: (1) uranium-series dating of coral from the Whiskey Run platform at Bandon, Oregon (Muhs et al., 1990); (2) aminostratigraphic correlation ages on mollusks from Cape Blanco (Muhs et al., 1990), Cape Arago (Muhs et al., 1990) and Yaquina Bay (Kennedy, 1978; Kennedy et al., 1982); and (3) degree of development and development stage assignments for soils in south coastal Oregon (Kelsey and Bockheim, 1994), at Cape Blanco (Bockheim et al., 1992), at Cape Arago (Bockheim et al., 1992), and along the central Oregon coast (Tables 2 and 3). A key observation that facilitated correlation using soil development was that there was generally a small increase in soil development on marine terrace deposits between the first two terraces followed by a significantly greater increase in development between the second and third terraces (Tables 3, 4, and 5) (Bockheim et al., 1992). Results of the terrace correlations are shown in Table 7; the correlations are the basis for our age assignments for the central Oregon terraces.

The lowest three central Oregon terraces have correlation ages of 80, 105, and 125 ka (Table 7). The numerical ages of these sea-level highstands are based on extensive studies of the chronology of late Pleistocene eustatic sea-level highstands (Mesolella et al., 1969; Bloom et al., 1974; Ku et al., 1974; Harmon et al., 1983; Chappell and Shackleton, 1986), and the ages correspond to oxygen isotope stages 5a, 5c, and 5e, respectively. Our assignment of terrace ages for the Yaquina Bay area, using correlation based on soils, is identical to that of Kennedy et al. (1982), who used aminostratigraphy.

For the central Oregon terraces older than stage 5, we assign minimum ages (Table 7) that are based on the chronology of pre-125 ka sea-level highstands that attained a height approximately equal to or greater than the sea-level elevation of the 125 ka highstand (+6 m) (Mesolella et al., 1969; Ku et al., 1974; Harmon et al., 1983). We speculate that the mini-

TABLE 5. SUMMARY OF SOIL PROPERTIES USED AS RELATIVE AGE INDICATORS IN THE YACHATS TO HECETA HEAD AREA (YACHATS BENCH)

Terrace locality	Parent material* (cm)	Bt horizon thickness	B horizon hue (cm)	Depth to Cox texture†	Maximum B horizon (% clay)†	Maximum estimated	Maximum clay films †	Development stage
GW3	Sand	49	10YR	120	cl	38	3n-mkpfpo	2
ST3	Sand	134	10YR	236	sicl	37	4kpfpo	4
RO3s	Sand	163	10YR	>230	sic	44	4mkpf	5
Average	Sand	115	10YR	>195	sicl	40	3-4mkpfpo	3.7
YNfa	Debris flow	>108	N.D.§	>152	sic	40	3mkpf	5
YNfb	Debris flow	240	N.D.§	>360	sicl	N.D.§	3mkpf	6
YNfc	Debris flow	100	N.D.§	>193	sicl	N.D.§	3kpf	5
YSf	Debris flow	168	7.5YR	280	sic	52	3kpf	5
GMf	Debris flow	78	10YR	>178	sic	52	4mk-kpf	4
RO3f	Debris flow	65	10YR	>270	sicl	40	4mkpf	4
Average	Debris flow	>127	10YR	>239	sic-cl	46	3–4mk-kpf	4.8

*Parent material for soils on the Yachats bench includes beach sand, dune sand, and debris flow deposits. The soil that formed on sand parent material on the Yachats bench has time-dependent properties comparable to the soil on the Yachats terrace to the north (Table 4 versus Table 5). Soil developed on debris flow deposits on the Yachats bench has greater Bt thicknesses and higher total clay contents than soil formed on beach deposits (Tables 4 and 5).

†See Table 2 for explanations.

§N.D., no data.

mum age for the Crestview terrace is 200 ka, because 200 ka is the approximate time prior to 125 ka when sea level was close to that at 125 ka. On the basis of the soil chronosequence and relative soil development along Reynolds Creek (near Reynolds Creek fault; Fig. 3), we infer that the Fern Ridge and Alder Grove terraces are considerably older than 200 ka.

We calculated uplift rates for platforms using the estimated elevation of the platform at the shoreline angle (Fig. 8) and the assigned platform ages (Table 7). To determine a range of possible elevations for the platform at the shoreline angle, we took the field-measured platform elevations and extrapolated them eastward to the shoreline angle using minimum and maximum platform gradients as defined by Bradley and Griggs (1976). We combined the range of possible shoreline-angle elevations with the North American model for paleo-sea-level data (Muhs, 1992; Muhs et al., 1992) to calculate a range of uplift magnitudes and uplift rates at specific shoreline-angle sites for the lowest three platforms (Table 8 and Fig. 8). Uncertainties assigned to the uplift-rate values (Table 8) incorporate uncertainties in both the pre-uplift and present-day elevation estimates for the shoreline angles.

LATE PLEISTOCENE CRUSTAL DEFORMATION AND COASTAL MORPHOLOGY

If upper-plate structures in central coastal Oregon have been active since 125 ka, topographic highs and lows along the coast could largely result from Quaternary tectonics and prominent embayments could be controlled by the structures.

Fault-Controlled Vertical Crustal Displacement, Cape Foulweather to Yaquina Bay

Faults near Cape Foulweather and at Yaquina Bay define a crustal block which, over the course of the late Quaternary, has been uplifted relative to the adjacent coastline (Figs. 8 and 9). The block is bounded to the south by Yaquina Bay and to the north by the lowland in the vicinity of Siletz Bay. The east-west faults that define this uplifted block include the Cape Foulweather fault to the north and the Yaquina Bay fault to the south (Figs. 3 and 9B).

We infer late Quaternary activity on a previously mapped fault, herein called the Cape Foulweather fault, from the displacement down to the north of the 125 ka and younger wave-cut platforms in the vicinity of Cape Foulweather (Fig. 8). As an alternative to a fault, it is possible that a crustal warp tilts platforms to the north. However, a fault mapped by Snavely et al. (1976c) in Tertiary sediment and basalt (Fig. 9B) has the correct position and sense of offset to be a candidate structure accounting for the platform deformation.

Shore-parallel profiles of platform elevations also show the magnitude of offset of the Yaquina Bay fault that cuts across Yaquina Bay (Fig. 8). The 125 ka Yachats platform is offset across Yaquina Bay in an up-to-the-north sense by 75 m, yielding a rate of vertical offset of 0.6 m/k.y. As a consequence, uplift rates north of Yaquina Bay between the Yaquina Bay and Cape Foulweather faults reach a maximum of 0.8 m/k.y., whereas on the south side of Yaquina Bay, uplift rates range from 0.1 to 0.4 m/k.y. (Table 8). Related minor faults are exposed north of Yaquina Bay at Nye Beach and Yaquina Head (Fig. 3); these faults offset the 80 ka Newport platform in the same north-side-up sense by 1.7 and 1.5 m, respectively.

The east-northeast–trending faults in the Cape Foulweather–Yaquina Bay region are almost perpendicular to the north-northwest–trending faults of the Waldport fault zone, situated farther south (Fig. 9). The east-west trend appears to be inherited from faults that cut the Paleogene rocks of the Coast Range (Snavely et al., 1976a, 1976b, 1976c). In contrast, the north-northwest trend of the Waldport fault zone is not parallel to any previously mapped fault trend, but is subparallel to bedding strike of the Tertiary marine sedimentary rocks.

Waldport Fault Zone and the Alsea Bay Downwarp

The Waldport fault zone trends ≈N12°E and consists of two main fault strands (Fig. 3). Both faults vertically displace marine terrace platforms, but the faults trend obliquely across the terrace back edges, thus it is difficult to assess the extent, if any, of strike-slip displacement of the paleo-sea cliffs. The dips of the faults are also unknown. The net vertical displacement along the Waldport fault zone is down on the east. The Waldport fault, the longest fault in the zone (≈14 km), extends obliquely across the Yachats-Crestview terrace contact and drops the Crestview terrace to about the same elevation as the younger Yachats terrace (Fig. 4, C and D). On the basis of the prefaulting elevation difference of these two platforms (determined where they are not separated by the Waldport fault; see Fig. 4B), we infer that the fault has accommodated at least 15–20 m of displacement down to the east since the time of cutting of the Yachats platform (125 ka). A fault subparallel to the Waldport fault (Reynolds Creek fault; Fig. 3) has a vertical displacement of 7 m opposite in sense to the Waldport fault (that is, up on the east); however, the fault is relatively short (≈0.9 km). The other fault strand is the Lint Slough fault (≥3.1 km long; Fig. 3), which also displaces platforms down to the east by ≈8–15 m across Lint Slough (Fig. 4D). Both the Waldport fault and the Lint Slough fault trend across Alsea Bay. Cumulative offset down to the east of the Waldport fault and the Lint Slough fault is greatest at the south margin of the bay, from which we infer that Alsea Bay is situated where the component of downthrow on the Waldport fault zone is the greatest. Minimum rates of vertical offset (down to the east) for the Waldport and Lint Slough faults are 0.1–0.15 and 0.07–0.1 m/k.y., respectively.

The influence of the Waldport fault zone on the development of Alsea Bay is further illumi-

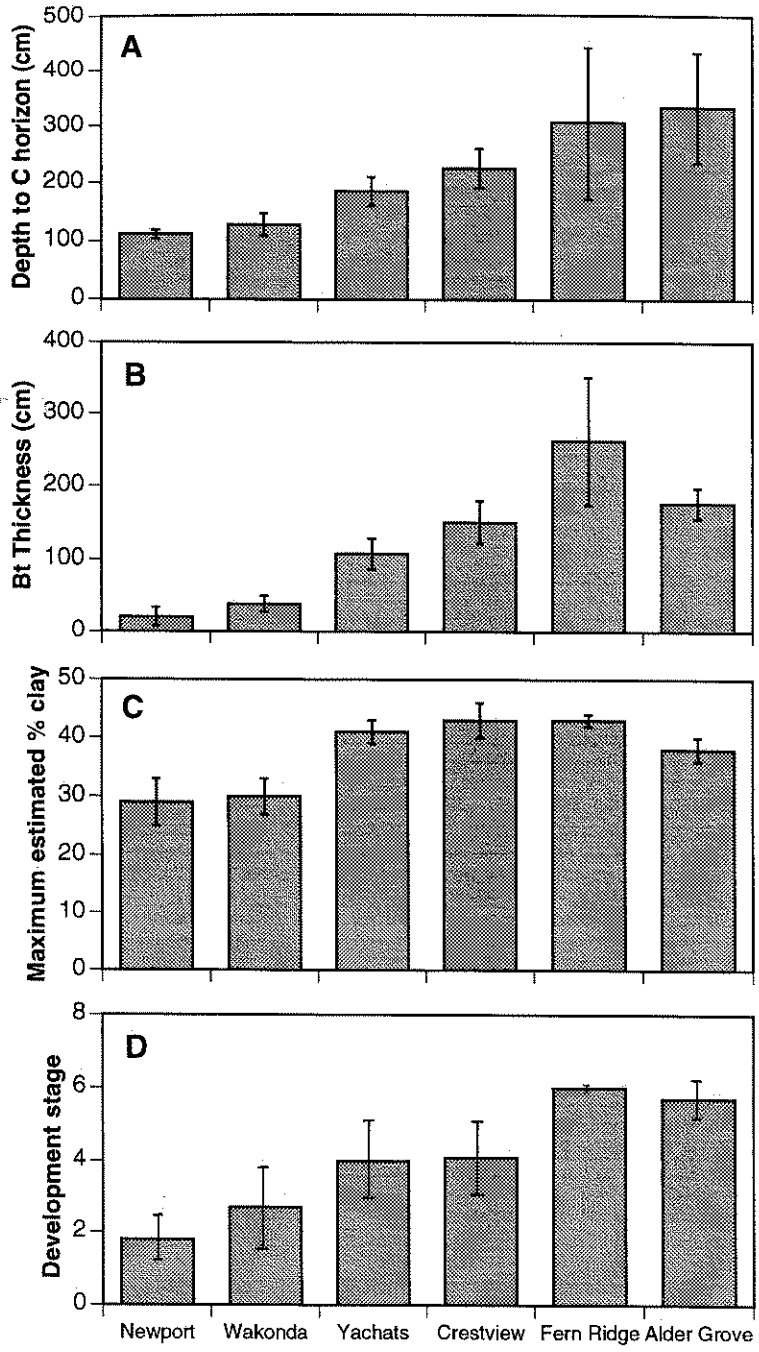

Figure 6. Charts showing average soil properties used as relative age indicators for soils developed on the six marine terraces. (A) Depth to C horizon. (B) Bt horizon thickness. (C) Estimated maximum percent clay in the Bt horizon. (D) Development stage (see Table 2). Vertical lines represent the standard error for the averages.

nated by deformation of the Crestview wave-cut platform, which is the only extensively preserved platform on the downthrown side of the Waldport fault zone. Shore-parallel profiles of platform elevation (Fig. 8) show that, in the vicinity of Alsea Bay, there is a crustal downwarp on the downthrown block of the Waldport fault defined by an uplift minimum for the Crestview platform (no. 4 platform; Fig. 8). The Alsea Bay downwarp (ABD; Fig. 8) is ≈4 km in wavelength, and the amplitude of the downwarp, considering the ±6 m elevation measurement error, is 14–37 m. Because the location of the downwarp is just east of the Waldport fault (Fig. 8), we infer that the Alsea Bay downwarp is a product of displacement on the Waldport fault zone. The inference that the 14–37 m amplitude downwarp is associated with the fault zone is consistent with the time of formation of the surface (the Crestview platform was cut ca. 200 ka) and the minimum rate of vertical offset of the Waldport fault (0.1–0.15 m/k.y.) during the late Pleistocene.

In conclusion, both of the major embayments, Yaquina Bay and Alsea Bay, appear to be structurally controlled by faults that have been active in the late Quaternary. Alsea Bay appears to straddle a region of downwarping on the downthrown side of the Waldport fault zone and Yaquina Bay rests on the downthrown block of the Yaquina Bay fault (Fig. 9).

South of Alsea Bay, uplift rates decrease to the south. For the 12 km coastal reach south of Yachats (Yachats bench) (Figs. 3 and 8), there has been little vertical displacement of the Yachats platform in the past 125 k.y. (data for lat 44.23°N to 44.28°N in Table 8). Thus, the Yachats bench is one of the few coastal segments along the Oregon and northern California portion of the Cascadia margin that records negligible net vertical crustal displacement since the last interglacial (125 ka). At Searose Beach at the southern end of the study area (Fig. 1), uplift rates reach a minimum of 0.00 to 0.04 m/k.y., calculated for the 125 ka platform (lat 44.23°N in Table 8).

DEFORMATION SINCE THE LATE PLEISTOCENE IN CENTRAL COASTAL OREGON

Deformation since the formation of the wave-cut platforms (since the late Pleistocene) is the result of many hundreds of cycles of interseismic and coseismic deformation. However, the paleoseismicity of upper-plate faults cannot be addressed through marine terrace studies. Although we know that these faults offset datums that are on the order of 100 ka in age and that the faults have a vertical component of slip rate of 0.1–0.6 m/k.y., no earthquakes have occurred on these faults since ca. 1870, and we do not know if these faults have the capability of rupturing independently of ruptures on the underlying megathrust or if these upper-plate faults could play a role in segmenting ruptures on the subduction zone.

Differences in the relative heights of benchmarks reoccupied by successive first-order leveling surveys provide a data set of historic, geodetically derived uplift rates along the coast for the past ≈45 yr, from 1941 to the releveling epoch 1987–1988 (Fig. 10) (Mitchell et al., 1994). Although the data are noisy because of

A. Elevations of marine platforms to north and south of Yaquina Bay (schematic).

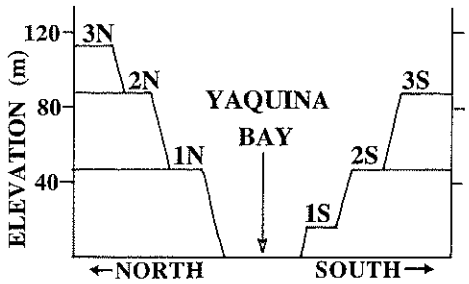

B. Possible matches and sense of fault offset based on platforms elevations (see A).

	1S	2S	3S
1N	NORTH SIDE UP I	NO OFFSET	SOUTH SIDE UP
2N	NORTH SIDE UP II	NORTH SIDE UP I	NO OFFSET
3N		NORTH SIDE UP II	NORTH SIDE UP I

C. Terrace matches based on soil data (Table 6) (solid = good match; shaded = possible match).

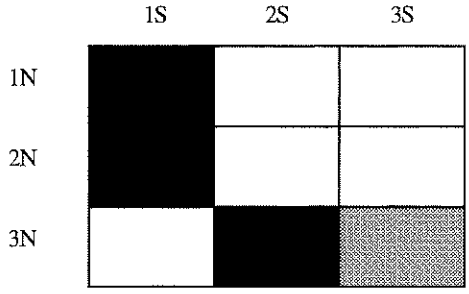

D. Displacement on Yaquina Bay fault using best platform match (match II in B).

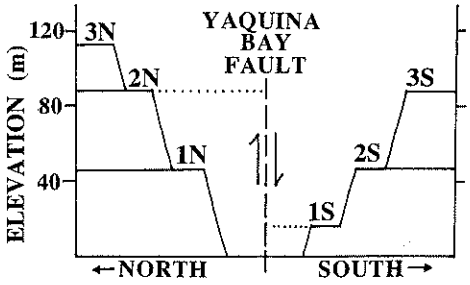

Figure 7. Diagrams describing how soil data are used to assess whether terrace surfaces are offset across Yaquina Bay. (A) Schematic cross section looking to east showing average elevation of wave-cut platforms on either side of Yaquina Bay; elevations are averaged over a 10 km distance to the north, or to the south, of the bay. (B) Matrix showing the possible terrace matches based on the terrace elevations in A; each matrix diagonal descending to the right represents a possible set of terrace matches—the type of offset required for each match is noted. (C) Matrix showing the terrace matches that are permissible based on soil data. A good match requires that the difference in soil development factors of the matched terraces is <1.0; a possible match indicates that the difference in soil development factors = 1.0. In the no match case (no shading), the difference in soil development factors is >1.0. (D) Preferred correlation of terraces across Yaquina Bay (the NORTH SIDE UP II match from B), schematically showing the magnitude of the up-to-the-north displacement on the Yaquina Bay fault.

TABLE 6. POSSIBLE TERRACE CORRELATIONS, BASED ON NUMERICAL DEVELOPMENT STAGE INDICES, FOR TERRACES ON EITHER SIDE OF YAQUINA BAY

Soil property*	Comparison with lowest terrace south of Yaquina Bay		Comparison with second lowest terrace south of Yaquina Bay		Comparison with third lowest terrace south of Yaquina Bay	
	Lowest south vs. lowest north†		Second-lowest south vs. lowest north		Third-lowest south vs. lowest north	
Bt horizon thickness (cm)	30	21	120	21	110	21
Depth to Cox (cm)	103	112	>210	112	>131	112
Max. estimated clay (%)	30	29	41	29	42	29
Development stage	2.5	1.8	4.5	1.8	4.3	1.8
	Lowest south vs. second-lowest north†		Second-lowest south vs. second-lowest north		Third-lowest south vs. second-lowest north	
Bt horizon thickness (cm)	32	>54	120	>54	110	>54
Depth to Cox (cm)	109	>168	>210	>168	>131	>168
Max. estimated clay (%)	N.D.	30	41	30	42	30
Development stage	2.5	3.0	4.5	3.0	4.3	3.0
	Lowest south vs. third-lowest north		Second-lowest south vs. third-lowest north†		Third-lowest south vs. third-lowest north†	
Bt horizon thickness (cm)	30	>212	120	>212	110	>212
Depth to Cox (cm)	103	>309	>210	>309	>131	>309
Max. estimated clay (%)	30	45	41	45	42	45
Development stage	2.5	5.3	4.5	5.3	4.3	5.3

Notes: Only soil sites located on terraces within 10 km north or south of Yaquina Bay are included in this table. Terraces north of Yaquina Bay are denoted 1N, 2N, and 3N; terraces south of Yaquina Bay are denoted 1S, 2S, and 3S. The numerical development stages (Kelsey and Bockheim, 1994) are averages using all sites on the specified terrace within the comparison area. N.D. = no data.

*Data from the following soils sites are included in this table: lowest terrace south = NS2, TH2, LC2; second-lowest terrace south = NS3, HC3, TH3, TC3; third-lowest terrace south = TH4, LC4, TC4; lowest terrace north = BB1, MC1, SP1, YH1; second-lowest terrace north = MC2, SP2, YH2, NN2; third-lowest-terrace north = MC3, NN3b, NN3c. These sites are described in greater detail in Tables 3, 4, and 5. In some cases, where thicknesses are preceeded by a > symbol, augering to 7 m depth failed to reach, or to penetrate through, the Cox horizon.

†Indicates terrace correlations that are possible, based on similar soil properties for the two terraces in question.

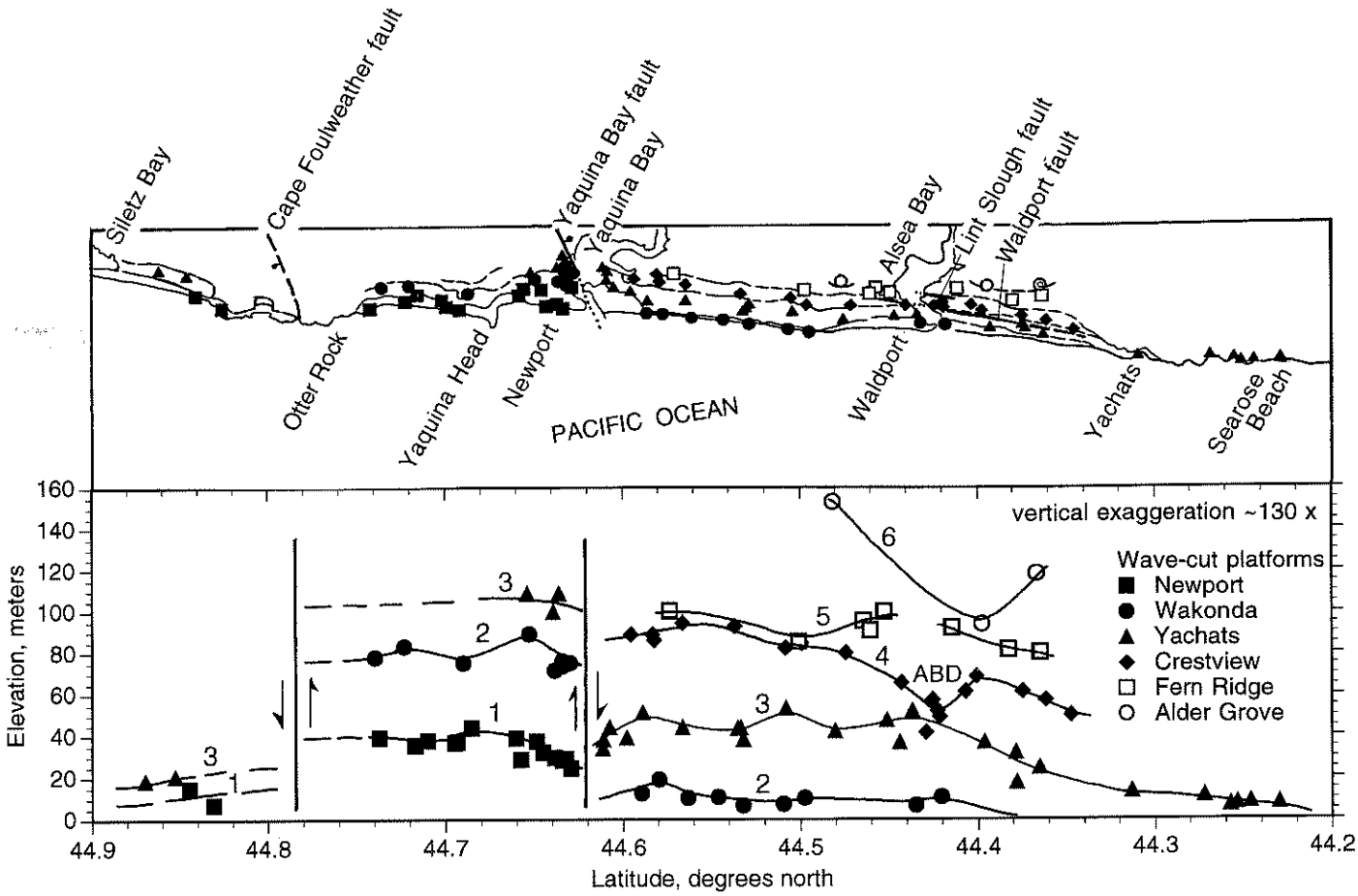

Figure 8. (Top) Map showing sites of platform elevation measurements and major faults. Lines that parallel the coastline are marine terrace paleo-sea cliffs: they are solid where well located and dashed where approximately located. (Bottom) View looking east showing the variations in the elevation of wave-cut platforms as projected onto a vertical plane trending north-south. The elevations in this profile are corrected to the equivalent shoreline angle elevations using the average platform gradient from Bradley and Griggs (1976) and using the shore-normal distance from the elevation measurement site to the back edge (shoreline angle) of the platform. ABD, Alsea Bay downwarp. Elevation measurement error is ±6 m and is represented by the symbol size.

TABLE 7. CORRELATION OF MARINE TERRACES ALONG THE SOUTHERN AND CENTRAL OREGON COAST

Central Oregon			South-Central Oregon						Southern Oregon*		
			Cape Arago†			Cape Blanco§					
Terrace	Assigned age (ka)	Development stage#	Terrace	Assigned age (ka)	Development stage#	Terrace	Assigned age (ka)	Development stage#	Terrace	Assigned age (ka)	Development stage#
Newport	80	1.8	Whiskey Run	80	1.0	Cape Blanco	80	1.4	Harris Beach	80	1.4
Wakonda	105	2.7	Pioneer	105	1.0	Pioneer	105	1.6	Brookings	105	2.4
Yachats	125	4.0	Seven Devils	125	3.8	Silver Butte	125	3.4	Gowman	125	3.1
Crestview	≥200	4.9	Metcalf	≥200	4.2	Indian Creek	≥200	3.6	Aqua Vista	≥200	5.1
Fern Ridge		6.0							Cornett		4.0
Alder Grove		5.7							Homestead		4.3
						Poverty Ridge		4.3	Alder Ridge		6.0

*Age assignments for southern Oregon marine terraces near Brookings reported in Kelsey and Bockheim (1994).
†Age assignments for Cape Arago marine terraces reported in Muhs et al. (1990) and McInelly and Kelsey (1990).
§Age assignments for Cape Blanco marine terraces reported in Kelsey (1990) and Muhs et al. (1990); correlation of Cape Blanco and Cape Arago marine terraces reported in Bockheim et al. (1992).
#For explanation of development stages for soils on marine terraces, see Table 2 and Kelsey and Bockheim (1994).

TABLE 8. UPLIFT RATES FOR WAVE-CUT PLATFORMS IN CENTRAL OREGON

Latitude (°N)	Marine terrace	Present elevation (m)*	Distance from back edge (m)	Elevation range adjusted to back edge (m)†	Age of platform (ka)	Paleo-high-stand elevation when platform was cut (m)§	Amount of surface uplift (min/max) (m)	Range of uplift rates (min/max) (m/k.y.)
North of Cape Foulweather fault								
44.845	Newport	3.5	285	9.2	80	–3	12.2	0.15
				14.9	80	–7	21.9	0.27
44.831	Newport	5.0	71	6.4	80	–3	9.4	0.12
				7.9	80	–7	14.9	0.19
44.870	Yachats	4.0#	655	14.4	125	6	8.4	0.07
				23.4	125	6	17.4	0.14
Between Cape Foulweather and Yaquina Bay faults								
44.686	Newport	34.2	357	41.3	80	–3	44.3	0.55
				48.5	80	–7	55.5	0.69
44.649	Newport	31.8	190	35.6	80	–3	38.6	0.48
				39.4	80	–7	46.4	0.58
44.723	Wakonda	75	262	80.2	105	–2	82.2	0.78
				85.5	105	–2	85.5	0.81
44.634	Wakonda	71.8	143	74.7	105	–2	74.7	0.71
				77.5	105	–2	79.5	0.76
44.654	Yachats	109	0	109	125	6	103	0.82
South of Yaquina Bay fault								
44.546	Wakonda	6.2	143	11.9	105	–2	13.9	0.13
				9.0	105	–2	11.0	0.10
44.498	Wakonda	4.3	202	12.4	105	–2	14.4	0.14
				8.3	105	–2	10.3	0.10
44.567	Yachats	30.9	536	40.1	125	6	34.1	0.27
				49.5	125	6	43.5	0.35
44.480	Yachats	25.8	762	46.0	125	6	40	0.32
				35.3	125	6	29.3	0.23
44.313	Yachats	4.5#	302	16.6	125	6	10.6	0.08
				10.5	125	6	4.5	0.04
44.23	Yachats	1.2#	238	10.7	125	6	4.7	0.04
				6.0	125	6	0	0.00

*Present elevation taken from topographic map and has precision of ±6 m.
†Elevation adjustment (a correction to a higher elevation) is 0.02–0.04 times distance to back edge for distances ≤450 m and 0.007–0.0017 times distance to back edge for distances >450 m; the adjustment accounts for the range of platform gradients cited in Bradley and Griggs (1976).
§Employing North American sea-level model (Muhs, 1992; Muhs et al., 1992): 105 ka sea level = –2 m; 80 ka sea level = –5 ± 2 m.
#Elevation surveyed to modern beach cliff and has precision of ±3 m.

slight vertical instabilities of individual benchmarks (see caption; Fig. 10), the trends in uplift rate derived from relative benchmark-elevation changes (dashed line; Fig. 10) are probably real and of tectonic origin, because analysis of independent tidal records along the same segment of coast (tide gages denoted by triangles in Fig. 10) yields the same magnitudes and trends in uplift (Mitchell et al., 1994).

The geodetically derived uplift rates are referenced to a contemporary sea-level rise of 1.8 ± 0.1 mm/yr (Douglas, 1991), with no correction for postglacial rebound. The uplift rates are several times larger and of opposite sign than the predicted magnitude of present-day postglacial forebulge collapse. The regional variation of uplift rate is also of a much shorter wavelength than that predicted for postglacial rebound effects (Tushingham and Peltier, 1992; Mitchell et al., 1994).

Historic, tide-gage–calibrated, geodetically derived uplift rates can be compared directly to wave-cut platform uplift rates because they are both uplift rates of rock as well as uplift rates of surfaces, erosion being insignificant at these sites over short periods of time. The ≈45 yr period may represent interseismic strain accumulation above a locked Cascadia subduction zone (Weldon, 1991; Mitchell et al., 1994), while the ≈125 k.y. period represents long-term, permanent vertical deformation of the upper plate. For the Oregon coast from the California-Oregon border north to lat 44°N (Fig. 2), uplift rates of wave-cut platforms averaged over the past 100 k.y. are relatively high along the same coastal zones where the 45 yr averaged vertical velocities of highway benchmarks are relatively high (Fig. 5 in Kelsey et al., 1994). A notable exception to this observation occurs along the central Oregon coast, where high uplift rates between Yaquina Bay and Cape Foulweather, averaged over the past 100 k.y., coincide with a notable lack of historic uplift of highway benchmarks over the same coastal length (Fig. 10). An explanation of this observation would contribute to understanding the seismotectonics of the central Oregon coast, but cannot be profitably pursued using only marine terrace deformation data and leveling data.

DISCUSSION

Marine terrace studies provide two data sets that bear on tectonics of the upper plate: uplift rates and distribution of faults and folds. We employ data on uplift rates and the distribution and character of upper-plate faults, in conjunction with previously published paleomagnetic data, to evaluate kinematic models of upper-plate deformation in Cascadia.

A significant aspect of the Tertiary and Quaternary structural history of the upper plate of the Cascadia subduction zone is the paleomagnetically documented rotation of crustal blocks, which was summarized by Wells and Heller (1988) and Wells (1990). All the rotation appears to postdate accretion of Tertiary rocks to the margin. The paleomagnetic data require as much as 80° of clockwise rotation for lower and middle Eocene oceanic basement that has been accreted to the Oregon and Washington continental margins. The best paleomagnetic data concerning rotations come from individual flows of the Miocene Columbia River Basalt Group, which show increasing rotation westward toward the coast for individual, chemically distinct basalt flows. Individual flows in western Washington and Oregon are rotated clockwise 15°–25° compared to the same flows on the Columbia Plateau. The amount of rotation in the Oregon Coast Range decreases in successively younger rocks at a rate of $\approx 1°/10^6$ yr (Beck and Plumley, 1980), and it also decreases northward from southern Oregon to the Columbia River (Fig. 4 in Wells, 1990). The size of the rotating crustal blocks is difficult to constrain in the poorly exposed, well-vegetated Coast Range; however, Wells and Coe (1985), on the basis of the most thorough structural study to date (in southwest Washington), inferred that the blocks may have bounds on the order of one to tens of kilometers and may rotate in part on fault systems inherited from previous episodes of tectonic deformation along the continental margin. Various workers (Beck, 1980; Wells et al., 1984; Engebretsen et al., 1985) inferred increasing dextral shear toward the deformation front of the Cascadia subduction zone on the basis of the paleomagnetic data, and attributed this shear to the long-term oblique subduction of the Farallon plate, and its present-day remnants, beneath the continental margin. England and Wells (1991) suggested that since the middle Miocene there has been as much as 15 mm/yr of northward translation of the west-

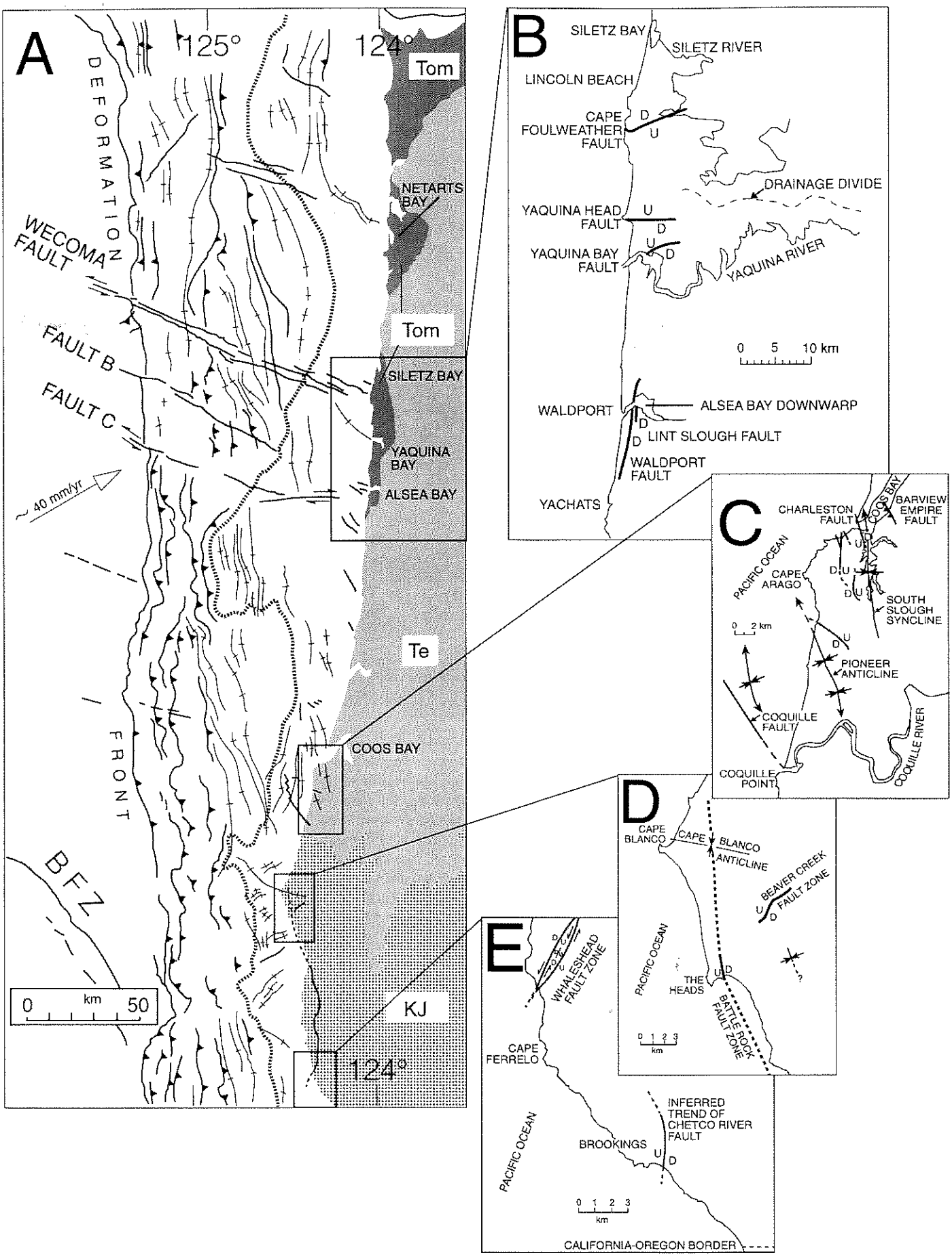
A
125°
124°
Tom
NETARTS BAY
DEFORMATION FRONT
WECOMA FAULT
FAULT B
FAULT C
Tom
SILETZ BAY
YAQUINA BAY
ALSEA BAY
~ 40 mm/yr
Te
COOS BAY
BFZ
0 km 50
KJ
124°
B
SILETZ BAY
SILETZ RIVER
LINCOLN BEACH
CAPE FOULWEATHER FAULT
D
U
DRAINAGE DIVIDE
YAQUINA HEAD FAULT
YAQUINA BAY FAULT
YAQUINA RIVER
0 5 10 km
WALDPORT
ALSEA BAY DOWNWARP
LINT SLOUGH FAULT
WALDPORT FAULT
YACHATS
C
CHARLESTON FAULT
COOS BAY
BARVIEW
EMPIRE FAULT
PACIFIC OCEAN
CAPE ARAGO
SOUTH SLOUGH SYNCLINE
0 2 km
PIONEER ANTICLINE
COQUILLE FAULT
COQUILLE RIVER
COQUILLE POINT
D
CAPE BLANCO
CAPE BLANCO ANTICLINE
BEAVER CREEK FAULT ZONE
PACIFIC OCEAN
THE HEADS
BATTLE ROCK FAULT ZONE
0 1 2 3 km
E
WHALESHEAD FAULT ZONE
CAPE FERRELO
PACIFIC OCEAN
INFERRED TREND OF CHETCO RIVER FAULT
BROOKINGS
0 1 2 3 km
CALIFORNIA-OREGON BORDER

Figure 9. (A) Summary tectonic map of the Oregon coast and offshore area (sources are Walker and MacLeod, 1991; Goldfinger et al., 1992b) showing more detailed tectonic maps for the following four coastal regions: (B) central Oregon coast; (C) Coos Bay–Cape Arago region (McInelly and Kelsey, 1990); (D) Cape Blanco region (Kelsey, 1990); and (E) southernmost coastal Oregon (Kelsey and Bockheim, 1994). All onshore structures have been active in the past 125 k.y. Bold lines are faults, and thin lines are synclines and anticlines.

ern continental margin, relative to stable North America, as a consequence of dextral shear and clockwise rotation.

Faults and folds that deform late Pleistocene wave-cut surfaces have been identified along three other segments of the Oregon coast, in addition to the central Oregon coast: Cape Arago–Coos Bay (McInelly and Kelsey, 1990); Cape Blanco (Kelsey, 1990); and Cape Ferrelo–Brookings (Kelsey and Bockheim, 1994) (Fig. 9, C, D, and E). Adjacent to the faults and folds, uplift rates are higher (≈0.4–1.0 m/k.y.) relative to the background rate of 0.0–0.2 m/k.y. (Kelsey and Bockheim, 1994).

The pattern of uplift and fault deformation in central coastal Oregon is the same as in the other coastal segments; wave-cut platforms between Yachats and Siletz Bay underwent a slow, long-term permanent uplift that averaged 0.1–0.3 m/k.y. in the late Pleistocene, with the exception of the fault-bounded block extending from Yaquina Bay to Cape Foulweather, where uplift rates approached 1 m/k.y. (Table 8). The Yaquina Bay fault bounds this block to the south and the Cape Foulweather fault bounds it to the north (Fig. 8). The zone of coastal faulting associated with this block is ≈20 km to the east of the eastern end of an east-southeast–trending fault zone, described by Goldfinger et al. (1992a, 1992b), that extends from the Cascadia deformation front across the continental slope and shelf to the coast (Fig. 9). The on-land faults and the faults on the shelf and slope project toward each other, but there are no data to suggest that they connect.

Within the 2- to 10-km-wide zone of marine terrace deformation in coastal Oregon, fold axes are variable in trend and the faults are diverse in trend and style from one coastal segment to the next, as well as within a single seg-

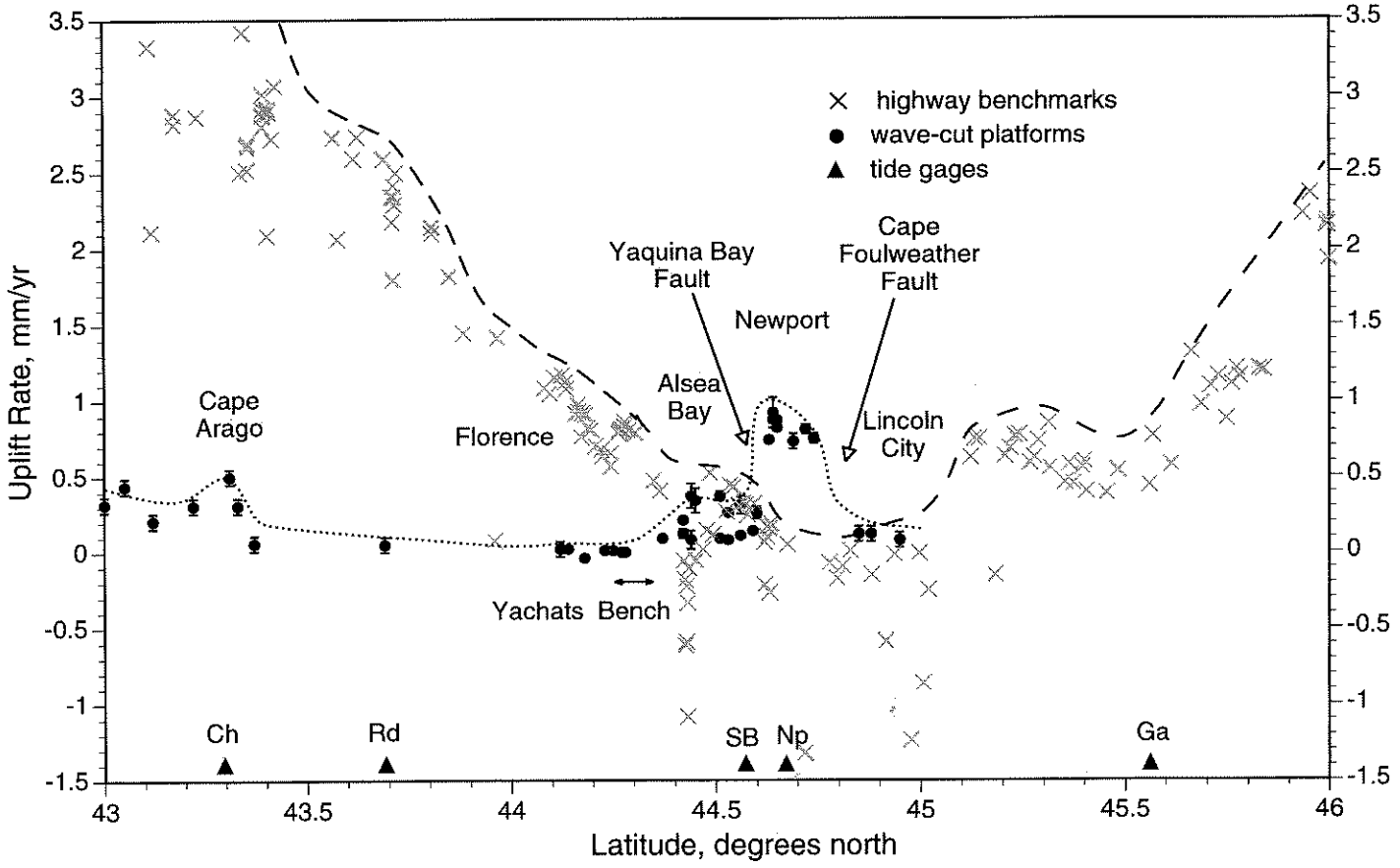

Figure 10. Along-coast variation in average uplift rates since 125 ka (solid dot symbol, derived from elevations and assigned ages for wave-cut platforms) versus uplift rates for 1941–1987 (× symbol, derived from releveling of highway benchmarks; Mitchell et al., 1994) for the central Oregon coast. Dotted line tracks the variation in average platform uplift rates. Dashed line delineates the upper limit for benchmark uplift rates. Triangles show locations of the tide gages that provide an independent check on the historic uplift rates from releveling. Some benchmarks yield uplift rates significantly below the upper limit, probably because of local subsidence, or settling, of individual benchmarks. Vertical bars represent range of platform uplift rates determined for the shoreline angle of the 80, 105, and 125 ka platforms using the minimum and maximum platform gradients from Bradley and Griggs (1976) and North American sea-level model (Muhs, 1992; Muhs et al., 1992) (see Table 8).

ment (Fig. 9). In southern Oregon, at Cape Blanco and Brookings (Fig. 9, D and E), active faulting along the north-northeast– to north-northwest–trending Whaleshead–Battle Rock fault zone occurs along a moderately or steeply dipping structure that sutures pre-Tertiary rock units within the Klamath Mountains. At Cape Blanco, the Cape Blanco anticline (Fig. 9D) trends perpendicular to the margin and has been actively growing since the Miocene (Kelsey, 1990). For the Whaleshead fault zone near Brookings (Fig. 9E), the ratio of sinistral strike slip to vertical offset is 5:1 (Kelsey and Bockheim, 1994). In all other cases, the relative importance of strike slip to vertical offset is unknown. Only in the Cape Arago area (Fig. 9C) do the faults appear to accommodate contraction parallel to the margin.

The many upper-plate structures having trends that are not parallel to the deformation front (Fig. 9) provide a basis for evaluating two kinematic models for the upper plate. Strike-slip faults can be the primary mechanism of margin-parallel transport in forearcs (e.g., see Fitch, 1972), but we infer that such a mechanism is not important in the upper plate of Cascadia because of the absence of strike-slip faults that parallel the deformation front. Rather, as has been suggested by numerous workers (i.e., England and Wells, 1991), we infer that dextral shear and clockwise rotation is a principle tectonic role of upper-plate faults and folds in coastal Oregon.

In deformation zones composed of rotating blocks, the block-bounding faults have a variety of trends and styles (examples for the western edge of the North American plate include Luyendyk et al., 1980; Jackson and Molnar, 1990; Wells and Coe, 1985). Upper-plate faults and folds in coastal Oregon also have a variety of trends and styles (Fig. 9, B–E), consistent with models for the Pacific Northwest proposed by Wells and Coe (1985) and Wells (1990), in which individual rotating blocks bounded by strike-slip faults make up a broad deformation zone undergoing clockwise rotation and dextral shear. This deformation zone extends from the coast to the Cascade arc; plate-boundary–related deformation extends eastward of the Cascade arc as well, into central Oregon (Pezzopane and Weldon, 1993).

Our contribution to this kinematic model is to identify numerous active structures along the coast that could accommodate both clockwise rotation and northward translation of the continental margin and to recognize that these structures are associated with localized uplift. We show a tectonic interpretation in which mapped faults in the central Oregon coast and adjacent offshore area accommodate clockwise rotation of discrete crustal blocks (Fig. 11). Figure 11 illustrates the hypothesized motion on structures and rotation of blocks of crust in the offshore area, as proposed by Goldfinger et al. (1992a), and supplements that hypothesis with a similar interpretation of fault deformation onshore.

Although the kinematic model of clockwise rotation and dextral shear has been proposed for both the offshore area and the onshore area, a tectonic boundary may exist between these two zones of deformation. On the basis of our mapping of wave-cut platform deformation, none of the major east-southeast–trending faults on the slope and shelf mapped by Goldfinger et al. (1992b) are present on the central Oregon coast in locations where they would project (Figs. 9 and 11). The Fulmar fault, a steeply dipping north-trending fault that is the western margin of the Eocene volcanic basement in the forearc (Snavely et al., 1980; Snavely, 1987), separates these two zones of deformation. On the basis of seismic records, Trehu et al. (1995) proposed that the fault is active and may decouple upper-plate deformation onshore from upper-plate deformation farther west offshore.

Because the onshore active fault zones coincide with localized high uplift rate along the coast (Fig. 8; Kelsey and Bockheim, 1994, Fig. 7), we infer that most upper-plate faults probably have a dip-slip component, as well as a strike-slip component. In most cases, the dip-slip component cannot be mapped in the field because of poor preservation of the faulted marine terraces. However, in the case of the Whaleshead fault zone (Fig. 9E), which has a sinuous trace over rugged topography, offset of the junction of the paleo-sea cliff and the wave-cut platform yields 2.5 m/k.y. of left-lateral

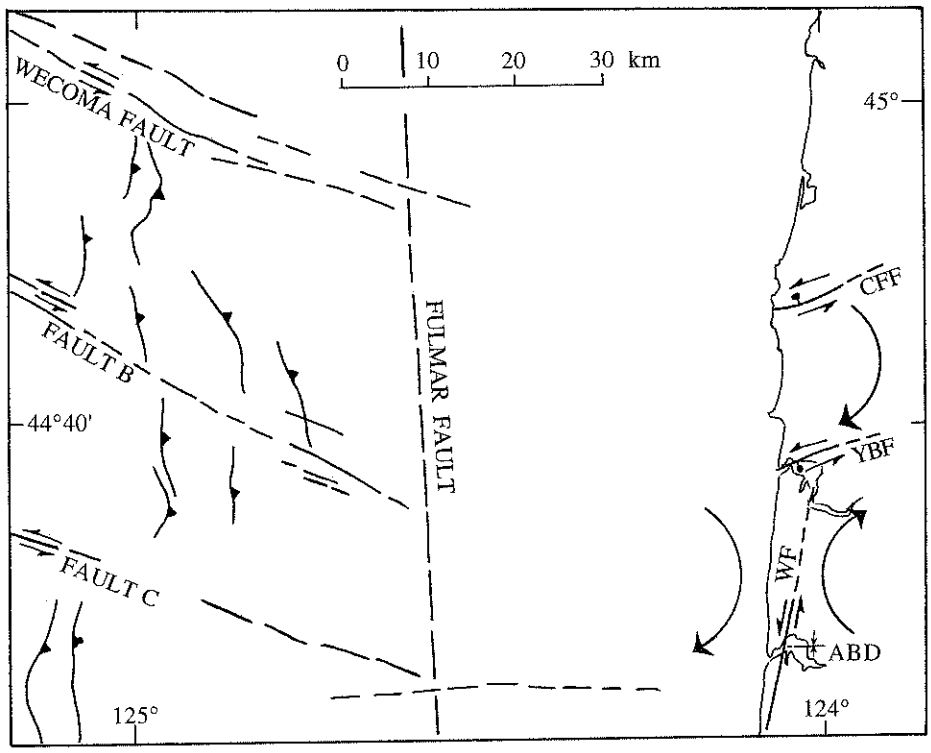

Figure 11. Interpretive tectonic map of a portion of the central Oregon coast and offshore continental shelf. Onshore structures: CFF, Cape Foulweather fault; YBF, Yaquina Bay fault; WF, Waldport fault; ABD, Alsea Bay downwarp. For the offshore, the map depicts those structures identified by Goldfinger et al. (1992b) as having been active since the Holocene or late Pleistocene (including Wecoma fault, Fault B and Fault C). Sense of motion indicators on the offshore faults are taken from Goldfinger et al. (1992b), who proposed rotation and dextral shear in the offshore deformation zone along these structures. We supplement that interpretation with a similar one for the onshore area, where geologic and geomorphic data permit but do not require a sinistral strike-slip component to the coastal faults. Also shown is the trace of the Fulmar fault (Fault A in Snavely et al., 1980; Snavely, 1987), which trends between the onshore and offshore zones of active faulting. On the basis of seismic reflection profiles, Trehu et al. (1995) suggested that the Fulmar fault is an active structure and may play a role in the partitioning of upper-plate strain.

strike slip and 0.5 m/k.y. of vertical slip since ca. 200 ka (Kelsey and Bockheim, 1994).

Measurements of crustal stress in the Oregon Coast Range may provide a means to evaluate the contention that most of the faults have a component of dip slip. If individual faults within a deformation zone that accommodates rotation are all purely strike slip, then rotation of a suite of adjoining blocks results in the centers of blocks moving away from each other along strike of the zone (Fig. 3 in Jackson and Molnar, 1990). However, it is unlikely that centers of crustal blocks are moving away from each other parallel to the north-south strike of the forearc deformation zone that includes the Oregon coast and the Coast Range. Numerous observations of contemporary stress in this region (Werner et al., 1991; Zoback, 1992), and the limited catalog of upper-plate earthquake focal mechanisms (Spence, 1989) indicate that the region is undergoing north-south compressional stress. North-south compressional stress is inconsistent with rotating crustal blocks moving away from each other within a north-south–trending deformation zone. It is also inconsistent with the rotation of crustal blocks along purely strike-slip faults, but is consistent with block-bounding faults having both a dip-slip and left-lateral strike-slip component (i.e., Jackson and Molnar, 1990). We conclude that because the blocks most likely rotate without moving away from each other, the block-bounding faults must accommodate both left-lateral strike-slip and dip-slip displacement. Whether the dip-slip displacement on individual upper-plate faults is contractional or extensional depends on the trend of the block-bounding fault relative to the north-south strike of the plate margin. Because of the variable trend of upper-plate faults along the coast (Fig. 9), probably only a portion of upper-plate faults accommodate contraction, and those that do accommodate contraction do not necessarily accommodate north-south contraction. Therefore, if north-south contraction of the forearc is occurring as a consequence of the observed north-south compressional stress, then a mechanism other than block rotation may be driving this contraction.

Considering that a major physiographic feature of the Cascadia subduction zone is the Coast Range with crest elevations 30–100 km east of the coast, is permanent uplift of the Coast Range being accommodated by upper-plate faults distributed throughout the ranges in the same manner that faults at the coast account for uplift of wave-cut platforms? Incision of late Pleistocene fluvial terraces along the major rivers that cut the Coast Range (Personius, 1993) implies that permanent uplift of the Coast Range has occurred since the late Pleistocene. Although candidate upper-plate faults occur throughout the Coast Range (Snavely et al., 1976a, 1976b, 1976c; Wells and Coe, 1985; Walsh et al., 1987; Walker and MacLeod, 1991; Wells et al., 1994), evaluation of their late Pleistocene or Holocene activity is in most (if not all) cases not possible because a suitable Pleistocene datum that could preserve cumulative offset is not present.

CONCLUSIONS

Marine terraces can serve as a datum to assess the character of surface uplift and faulting along the Oregon coast since the late Pleistocene. Using this data set, we explore the nature of upper-plate deformation along the Oregon portion of the Cascadia subduction zone. Coastal uplift rates are in general low, on the order of 0.1–0.3 m/k.y. Long-term subsidence is not the norm, nor are long-term uplift rates $\geq\approx$0.4 m/k.y. However, along coastal reaches of limited extent (on the order of 8–13 km in coastwise length), uplift rates approach 1.0 m/k.y. These reaches of high uplift rate are coincident with mappable faults and folds in the upper plate.

In an attempt to better understand upper-plate deformation in the late Quaternary, we evaluated all faults and folds in southern and central coastal Oregon that displace wave-cut platforms and account for anomalies of high uplift rate. Fold axes are variable in trend and faults are diverse in trend and style from one coastal segment to the next, as well as within a single segment. The pattern and type of faulting are consistent with a model, suggested previously by numerous workers, in which the upper-plate deformation zone at the continental margin of the Pacific Northwest is undergoing clockwise rotation and dextral shear by rotation of individual blocks along block-bounding faults.

Our contribution to this working model is to identify numerous coastal structures that could be block-bounding faults. These faults would accommodate clockwise rotation through left-lateral strike-slip displacement. Because these faults account for localized uplift, the faults probably also have a dip-slip component. Displacement of wave-cut platforms along the Whaleshead fault zone in southern Oregon supports the inference of oblique-slip faults: the ratio of horizontal to vertical slip (uplift) since the late Pleistocene on this fault is 5:1, with 2.5 m/k.y. of left-lateral displacement and 0.5 m/k.y. of vertical displacement. Block-bounding, oblique-slip, upper-plate faults in coastal Oregon, such as the Whaleshead fault zone, may accommodate either contraction or extension, depending on the orientation of the fault relative to the north-south trend of the plate margin.

Permanent uplift of the Coast Range could be accommodated by upper-plate faults similar to those documented along the coastal zone. Although numerous candidate faults have been mapped throughout the Coast Range, the ranges, unlike the coast, lack the preservation of a widespread Pleistocene surface that could record cumulative displacement during the Quaternary.

ACKNOWLEDGMENTS

This research was supported by National Science Foundation grant EAR-8903470 to Kelsey and Bockheim. We thank J. G. Marshall for field assistance and C. Goldfinger, L. McNeill, and R. E. Wells for helpful discussions. This paper was improved through reviews by B. F. Atwater, E. D. Humphreys, M. Lisowski, E. R. Schermer, and R. E. Wells.

REFERENCES CITED

Adams, J., 1984, Active deformation of the Pacific Northwest continental margin: Tectonics, v. 3, p. 449–472.

Applegate, B., Goldfinger, C., MacKay, M. E., Kulm, L. D., Fox, C. G., Embley, R. W., and Meis, P. J., 1992, A left-lateral strike-slip fault seaward of the Oregon convergent margin: Tectonics, v. 11, p. 465–477.

Atwater, B. F., 1987, Evidence for great Holocene earthquakes along the outer coast of Washington State: Science, v. 236, p. 942–944.

Atwater, B. F., 1992, Geologic evidence for earthquakes during the past 2000 years along the Copalis River, southern coastal Washington: Journal of Geophysical Research, v. 97, p. 1901–1919.

Atwater, B. F., and 15 others, 1995, Summary of coastal geologic evidence for past great subduction earthquakes at the Cascadia subduction zone: Earthquake Spectra, v. 11, p. 1–18.

Beck, M. E., 1980, Paleomagnetic record of plate-margin tectonic processes along the western edge of North America: Journal of Geophysical Research, v. 85, p. 7115–7131.

Beck, M. E., and Plumley, P. W., 1980, Paleomagnetism of intrusive rocks in the Coast Range of Oregon: Microplate rotation in middle Tertiary time: Geology, v. 8, p. 573–577.

Bloom, A. L., Broeker, W. S., Chappell, M. M. A., Matthews, R. K., and Mesolella, K. J., 1974, Quaternary sea level fluctuations on a tectonic coast: New $^{230}Th/^{234}U$ dates from the Huon Peninsula, New Guinea: Quaternary Research, v. 4, p. 185–205.

Bockheim, J. G., Kelsey, H. M., and Marshall, J. G., 1992, Soil development, relative dating, and correlation of late Quaternary marine terraces in southwestern Oregon: Quaternary Research, v. 37, p. 60–74.

Bradley, W. C., and Griggs, G. B., 1976, Form, genesis, and deformation of central California wave-cut platforms: Geological Society of America Bulletin, v. 87, p. 433–449.

Chappell, J., and Shackleton, N. J., 1986, Oxygen isotopes and sea level: Nature, v. 324, p. 137–140.

Clague, J. J., and Bobrowsky, P. T., 1994, Evidence for a large earthquake and tsunami 100–400 years ago on western Vancouver Island, British Columbia: Quaternary Research, v. 41, p. 176–184.

Clarke, S. H., and Carver, G. A., 1992, Late Holocene tectonics and paleoseismicity, southern Cascadia subduction zone: Science, v. 225, p. 188–192.

Darienzo, M. E., 1991, Late Holocene paleoseismicity along the northern Oregon coast [Ph.D. thesis]: Portland, Oregon, Portland State University, 167 p.

Darienzo, M. E., and Peterson, C. D., 1990, Episodic tectonic subsidence of late Holocene salt marshes, northern Oregon central Cascadia margin: Tectonics, v. 9, p. 1–22.

Darienzo, M. E., Peterson, C. D., and Clough, C., 1994, Stratigraphic evidence for great subduction zone earthquakes in four estuaries in northern Oregon, U.S.A.: Journal of Coastal Research, v. 10, p. 850–876.

Douglas, B. C., 1991, Global sea level rise: Journal of Geophysical Research, v. 96, p. 6981–6992.

Engebretson, D. C., Cox, A., and Gordon, R. G., 1985, Relative motions between oceanic and continental plates in the Pacific basin: Geological Society of America Special Paper 206, 59 p.

England, P., and Molnar, P., 1990, Surface uplift, uplift of rocks, and exhumation of rocks: Geology, v. 18, p. 1173–1177.

England, P., and Wells, R. E., 1991, Neogene rotations and quasicontinuous deformation of the Pacific Northwest continental margin: Geology, v. 19, p. 978–981.

Fitch, T. J., 1972, Plate convergence, transcurrent faults and internal deformation adjacent to southeast Asia and the western Pacific: Journal of Geophysical Research, v. 77, p. 4432–4460.

Goldfinger, C., Kulm, L. D., Yeats, R. S., Appelgate, B., MacKay, M. E., and Moore, G. F., 1992a, Transverse structural trends along the Oregon convergent margin: Implications for Cascadia earthquake potential and crustal rotations: Geology, v. 20, p. 141–144.

Goldfinger, C., and eight others, 1992b, Neotectonic map of the Oregon continental margin and adjacent abyssal plain: Oregon Department of Geology and Mineral Industries Open-File Report 0-92-4, 17 p.

Griggs, A. B., 1945, Chromite-bearing sands of the southern part of the coast of Oregon: U.S. Geological Survey Bulletin 945-E, p. 113–150, 11 pl.

Harmon, R. S., and eight others, 1983, U-series and amino-acid racemization geochronology of Bermuda—Implications for eustatic sea level fluctuations over the past 250,000 years: Palaeogeography, Palaeoclimatology, Palaeoecology, v. 44, p. 41–70.

Jackson, J., and Molnar, P., 1990, Active faulting and block rotations in the western Transverse Ranges, California: Journal of Geophysical Research, v. 95, p. 22073–22087.

Janda, R. J., 1969, Age and correlation of marine terraces near Cape Blanco, Oregon: Geological Society of America Abstracts with Programs, v. 3, p. 29–30.

Kelsey, H. M., 1990, Late Quaternary deformation of marine terraces on the Cascadia subduction zone near Cape Blanco, Oregon: Tectonics, v. 9, p. 983–1014.

Kelsey, H. M., and Bockheim, J. G., 1994, Coastal landscape evolution as a function of eustasy and surface uplift, southern Cascadia margin, USA: Geological Society of America Bulletin, v. 106, p. 840–854.

Kelsey, H. M., Witter, R. C., and Polenz, M., 1993, Cascadia paleoseismic record derived from late Holocene fluvial and lake sediments, Sixes River Valley, Cape Blanco, south coastal Oregon: Eos (Transactions, American Geophysical Union), v. 74, p. 199.

Kelsey, H. M., Engebretson, D. C., Mitchell, C. E., and Ticknor, R. L., 1994, Topographic form of the Coast Ranges of the Cascadia margin in relation to coastal uplift rates and plate subduction: Journal of Geophysical Research, v. 99, p. 12245–12255.

Kennedy, G. L., 1978, Pleistocene paleoecology, zoogeography and geochronology of marine invertebrate faunas of the Pacific Northwest coast (San Francisco Bay to Puget Sound) [Ph.D. thesis]: Davis, University of California, 824 p.

Kennedy, G. L., Lajoie, K. R., and Wehmiller, J. F., 1982, Aminostratigraphy and faunal correlations of late Quaternary marine terraces: Science, v. 299, p. 545–547.

Ku, T. L., Kimmel, M. A., Easton, W. H., and O'Neil, T. J., 1974, Eustatic sea level 120,000 years ago on Oahu, Hawaii: Science, v. 183, p. 959–962.

Kulm, L. D., and Fowler, G. A., 1974, Oregon continental margin structure and stratigraphy: A test of the imbricate thrust model, *in* Burk, C. A., and Drake, C. L., eds., The geology of continental margins: New York, Springer-Verlag, p. 261–284.

Lajoie, K. R., 1986, Coastal tectonics, *in* Wallace, R. E., et al., eds., Active tectonics: Washington, D.C., National Academy Press, p. 95–124.

Luyendyk, B. P., Kamerling, M. J., and Terres, R., 1980, Geometric model for Neogene crustal rotation in southern California: Geological Society of America Bulletin, v. 91, p. 211–217.

McInelly, G. W., and Kelsey, H. M., 1990, Late Quaternary tectonic deformation in the Cape Arago–Bandon region of coastal Oregon as deduced from wave-cut platforms: Journal of Geophysical Research, v. 95, p. 6699–6713.

Merritts, D., and Bull, W. B., 1989, Interpreting Quaternary uplift rates at the Mendocino triple junction, northern California, from uplifted marine terraces: Geology, v. 17, p. 1020–1024.

Mesolella, K. J., Matthews, R. K., Broecker, W. S., and Thurber, D. L., 1969, The astronomical theory of climatic change: Barbados data: Journal of Geology, v. 77, p. 250–274.

Mitchell, C. E., Vincent, P., Weldon, R. J., and Richards, M. A., 1994, Present-day vertical deformation of the Cascadia margin, Pacific Northwest, United States: Journal of Geophysical Research, v. 99, p. 12257–12278.

Muhs, D. R., 1992, The last interglacial-glacial transition in North America: Evidence from uranium-series dating of coastal deposits, *in* Clark, P. U., and Lea, P. D., eds., The last interglacial-glacial transition in North America: Geological Society of America Special Paper 270, p. 31–51.

Muhs, D. R., Kelsey, H. M., Miller, G. H., Kennedy, G. L., Whelan, J. F., and McInelly, G. W., 1990, Age estimates and uplift rates for late Pleistocene marine terraces; southern Oregon portion of the Cascadia forearc: Journal of Geophysical Research, v. 95, p. 6685–6689.

Muhs, D. R., Rockwell, T. K., and Kennedy, G. L., 1992, Late Quaternary uplift rates of marine terraces on the Pacific Coast of North America, southern Oregon to Baja California Sur: Quaternary International, v. 15/16, p. 121–133.

Nelson, A. R., 1992, Holocene tidal-marsh stratigraphy in south-central Oregon—Evidence for localized sudden submergence in the Cascadia subduction zone: Society for Sedimentary Geology (SEPM) Special Publication 48, p. 287–301.

Personius, S. F., 1993, Age and origin of fluvial terraces in the central Coast Range, western Oregon: U.S. Geological Survey Bulletin 2038, 56 p.

Peterson, C. D., and Darienzo, M., 1988, Episodic tectonic subsidence of late Holocene salt marshes in Oregon: Clear evidence of abrupt strain release and gradual strain accumulation in the southern Cascadia margin during the last 3,500 years: U.S. Geological Survey Open-File Report 88-0541, 3 p.

Peterson, C. D., and Darienzo, M., 1990, Evidence of subduction zone paleoseismicity from the central Oregon margin, Alsea Bay, Oregon [abs.]: Eos (Transactions, American Geophysical Union), v. 71, p. 1069.

Peterson, C. D., and Darienzo, M., 1996, Discrimination of climatic, oceanic, and tectonic mechanisms of cyclic marsh burial from Alsea Bay, Oregon, U.S.A., *in* Rodgers, A. M., Kockelman, W. J., Priest, G., and Walsh, T. J., eds., Assessing and reducing earthquake hazards in the Pacific Northwest: U.S. Geological Survey Professional Paper 1560, in press.

Peterson, C. P., Kulm, L. D., and Gray, J. J., 1986, Geologic map of the ocean floor off Oregon and the adjacent continental margin: Oregon Department of Geology and Mineral Industries Map GMS-42, scale 1:500 000.

Pezzopane, S. K., and Weldon, R. J., 1993, Tectonic role of active faulting in central Oregon: Tectonics, v. 12, p. 1140–1169.

Riddihough, R., 1984, Recent movements of the Juan de Fuca plate system: Journal of Geophysical Research, v. 89, p. 6980–6994.

Snavely, P. D., Jr., 1987, Tertiary geologic framework, neotectonics, and petroleum potential for the Oregon-Washington continental margin, *in* Scholl, D. W., Grantz, A., and Vedder, J. G., eds., Geology and resource potential of the continental margin of western North America and adjacent ocean basins—Beaufort Sea to Baja California: Houston, Texas, Circum-Pacific Council for Energy and Mineral Resources, Earth Science Series, v. 6, p. 305–335.

Snavely, P. D., Jr., MacLeod, N. S., and Rau, W. W., 1969, Geology of the Newport area, Oregon: The Ore Bin, v. 31, p. 25–48.

Snavely, P. D., Jr., MacLeod, N. S., Wagner, H. C., and Rau, W. W., 1976a, Geologic map of the Waldport and Tidewater quadrangles, Lincoln, Lane, and Benton Counties, Oregon: U.S. Geological Survey Miscellaneous Geologic Investigations Map I-866, scale 1:62 500.

Snavely, P. D., Jr., MacLeod, N. S., Wagner, H. C., and Rau, W. W., 1976b, Geologic map of the Yaquina and Toledo quadrangles, Lincoln County, Oregon: U.S. Geological Survey Miscellaneous Geologic Investigations Map I-867, scale 1:62 500.

Snavely, P. D., Jr., MacLeod, N. S., Wagner, H. C., and Rau, W. W., 1976c, Geologic map of the Cape Foulweather and Euchre Mountain quadrangles, Lincoln County, Oregon: U.S. Geological Survey Miscellaneous Geologic Investigations Map I-868, scale 1:62 500.

Snavely, P. D., Jr., Wagner, H. C., and Lander, D. L., 1980, Geologic cross section of the central Oregon continental margin: Geological Society of America Map and Chart Series MC-28J, scale 1:250 000.

Soil Survey Staff, 1975, Soil taxonomy: A basic system of soil classification for making and interpreting soil surveys: Washington D.C., U.S. Department of Agriculture, Soil Conservation Service, Agricultural Handbook 436.

Spence, W., 1989, Stress origins and earthquake potentials in Cascadia: Journal of Geophysical Research, v. 94, p. 3076–3088.

Ticknor, R. L., 1993, Late Quaternary crustal deformation on the central Oregon coast as deduced from uplifted wave-cut platforms [M.S. thesis]: Bellingham, Western Washington University, 70 p.

Trehu, A. M., Lin, G., Maxwell, E., and Goldfinger, C., 1995, A seismic reflection profile across the Cascadia subduction zone offshore central Oregon: New constraints on methane distribution and crustal structure: Journal of Geophysical Research, v. 100, p. 15101–15116.

Tushingham, A. M., and Peltier, W. R., 1992, Validation of the ICE-3G model of Würm-Wisconsin deglaciation using a global data base of relative sea level histories: Journal of Geophysical Research, v. 97, p. 3285–3304.

Walker, G. W., and MacLeod, N. S., 1991, Geologic map of Oregon: U.S. Geological Survey Special Geologic Maps, 2 sheets, scale 1:500 000.

Walsh, T. J., Korosec, M. A., Phillips, W. M., Logan, R. L., and Schasse, H. W., 1987, Geologic map of Washington—Southwest quadrant: Washington State Department of Natural Resources Geologic Map GM-34, scale 1:250 000.

Weldon, R. J., II, 1991, Active tectonic studies in the United States, 1987–1990: U.S. Natl. Rep. Int. Union Geol. Geophys. 1987–1990: Reviews in Geophysics, v. 29, p. 890–906.

Wells, R. E., 1990, Paleomagnetic rotations and the Cenozoic tectonics of the Cascade arc, Washington, Oregon and California: Journal of Geophysical Research, v. 95, p. 19409–19417.

Wells, R. E., and Coe, R. S., 1985, Paleomagnetism and geology of Eocene volcanic rocks of southwest Washington, implications for mechanisms of tectonic rotation: Journal of Geophysical Research, v. 90, p. 1925–1947.

Wells, R. E., and Heller, P. L., 1988, The relative contribution of accretion, shear and extension to Cenozoic tectonic rotation in the Pacific Northwest: Geological Society of America Bulletin, v. 100, p. 325–338.

Wells, R. E., Engebretson, D. C., Snavely, P. D., Jr., and Coe, R. S., 1984, Cenozoic plate motions and the volcano-tectonic evolution of western Oregon and Washington: Tectonics, v. 3, p. 275–294.

Wells, R. E., Snavely, P. D., Jr., MacLeod, N. S., Kelly, M. M., and Parker, M. J., 1994, Geologic map of the Tillamook Highlands, northwest Oregon Coast Range: U.S. Geological Survey Open-File Report 94-21, scale 1:62 500.

Werner, K. S., Graven, E. P., Berkman, T. A., and Parker, M. J., 1991, Direction of maximum horizontal compression in western Oregon determined by borehole breakouts: Tectonics, v. 10, p. 948–958.

Zoback, M. L., 1992, First- and second-order patterns of stress in the lithosphere: The world stress map project: Journal of Geophysical Research, v. 97, p. 11703–11728.

MANUSCRIPT RECEIVED BY THE SOCIETY DECEMBER 23, 1994
REVISED MANUSCRIPT RECEIVED SEPTEMBER 29, 1995
MANUSCRIPT ACCEPTED NOVEMBER 15, 1995

Printed in U.S.A.